View metadata, citation and similar papers at core.ac.uk

brought to you by CORE

provided by Online Research Database In Technology

Technical University of Denmark

Polymers for Insulin Reservoirs and Delivery Systems

Fristrup, Charlotte Juel; Hvilsted, Søren; Jankova Atanasova, Katja ; Eskimergen, Rüya

Publication date:
2011

Document Version
Publisher's PDF, also known as Version of record

Link back to DTU Orbit

Citation (APA):
Fristrup, C. J., Hvilsted, S., Jankova Atanasova, K., & Eskimergen, R. (2011). Polymers for Insulin Reservoirs and Delivery Systems. Kgs. Lyngby, Denmark: Technical University of Denmark (DTU).

DTU Library
Technical Information Center of Denmark

General rights
Copyright and moral rights for the publications made accessible in the public portal are retained by the authors and/or other copyright owners and it is a condition of accessing publications that users recognise and abide by the legal requirements associated with these rights.

- Users may download and print one copy of any publication from the public portal for the purpose of private study or research.
- You may not further distribute the material or use it for any profit-making activity or commercial gain
- You may freely distribute the URL identifying the publication in the public portal

If you believe that this document breaches copyright please contact us providing details, and we will remove access to the work immediately and investigate your claim.

Polymers for Pharmaceutical Packaging and Delivery Systems

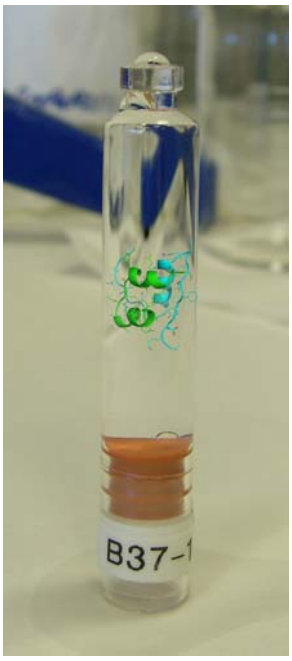

Charlotte Juel Fristrup
PhD Thesis
2010

DTU Chemical Engineering
Department of Chemical and Biochemical Engineering

Contents

List of Abbreviations

AA	Acrylic acid
AAm	Acrylamide
Aβ	Amyloid-β
AFM	Atomic force microscopy
AGET	Activators generated by electron transfer
ARGET	Activator regenerated by electron transfer
AsA	L-Ascorbic acid
Asp^{B28} insulin	Insulin aspart
ATR-FTIR	Attenuated total reflectance fourier transform infrared
ATRP	Atom transfer radical polymerization
*t*BA	*tert*-Butyl acrylate
*t*BAEMA	2-(*tert*-Butylamino)ethyl methacrylate
Bipy	2,2'-Bipyridine
BP-*i*-BuBr	Benzophenonyl bromoisobutyrate
Br-*i*-BuBr	2-Bromoisobutyryl bromide
BSA	Bovine serum albumin
CBMA	2-Carboxy-*N*,*N*-dimethyl-*N*-(2'-methacryloyloxyethyl)ethanaminium inner salt
CFRP	Conventional free radical polymerization
o-DCB	*ortho*-Dichlorobenzene
DEAEMA	2-(Diethylamino)ethyl methacrylate
DMAAm	*N*,*N*-Dimethylacrylamide
DMAEMA	2-(*N*,*N*-Dimethylamino)ethyl methacrylate
DMDP	4,4'-Dimethyl-2,2'-dipyridyl
DMF	*N*,*N*-Dimethyl formamide
DMSO	Dimethyl sulfoxide
DPC	Danish polymer centre
DTU	Technical university of Denmark
DVB	Divinylbenzene
EDC	1-Ethyl-3-(3-dimethylaminopropyl)-carbodiimide hydrochloride
EO	Ethylene oxide
FESEM	Field emission scanning electron microscope
GMA	Glycidyl methacrylate
GMMA	Glycerol monomethacrylate
HEMA	2-Hydroxyethyl methacrylate
HMTETA	1,1,4,7,10,10-Hexamethyltriethylenetetramine
HMWP	Higher molecular weight proteins
HPLC	High performance liquid chromatography
ICP-OES	Inductive coupled plasma optical emission spectroscopy
LCST	Lower critical solution temperature
MAAS	Methacrylic acid sodium salt
MAIpGlc	3-*O*-Methacryloyl-1,2:5,6-di-*O*-isopropylidene-D-glucofuranose

MCF	Mesostructured cellular foam
Me_4Cyclam	1,4,8,11-Tetraazacyclotetradecane
MEMA	2-Methoxyethyl methacrylate
Me_6TREN	Tris(2-(dimethylamino)ethyl)amine
MMA	Methyl methacrylate
MPC	2-Methacryloyloxyethyl phosphorylcholine
MPDSAH	(3-(Methacryloylamino)propyl)-dimethyl(3-sulfopropyl) ammonium hydroxide
MPEG	Monomethoxy poly(ethylene glycol)
MPEGMA	Poly(ethylene glycol)methyl ether methacrylate
NIPAAm	*N*-Isopropylacrylamide
NMP	1-Methyl-2-pyrrolidione
NP	Nanoparticle
PDMS	Poly(dimethylsiloxane)
PEEK	Poly(ether ether ketone)
PEG	Poly(ethylene glycol)
PEGMA	Poly(ethylene glycol) methacrylate
PET	Poly(ethylene terephthalate)
PI	Polyimide
PMDETA	1,1,4,7,7-Pentamethyldiethylenetriamine
PP	Polypropylene
pp-MPEGMA	plasma-polymerized poly(ethylene glycol)methyl ether methacrylate
PS	Polystyrene
PTFE	Poly(tetrafluoroethylene)
PVBC	Poly(4-vinylbenzyl chloride)
PVDF	Poly(vinylidene fluoride)
QCM	Quartz crystal microbalance
RP	Reverse phase
SAIs	Surface anchored initiators
SBMA	Sulfobetaine methacrylate
SEC	Size exclusion chromatography
SEM	Scanning electron microscope
SI-ATRP	Surface-initiated atom transfer radical polymerization
SP	(-)-Sparteine
SPM	3-Sulfopropyl methacrylate potassium salt
SPR	Surface plasmon resonance
TEA	Triethylamine
TGA	Thermal gravimetric analysis
THF	Tetrahydrofuran
UV	Ultraviolet
2-VP	2-Vinylpyridine
4-VP	4-Vinylpyridine
WCA	Water contact angle
XPS	X-ray photoelectron spectroscopy

1 Background

Storage and administration of protein drugs are imperative in modern society. Glass is used for storage of protein drugs; however, the material is fragile and does not offer design of freedom for products in a mass production. If polymers could replace glass it will make a difference. Polymers will especially be suitable for devices with demands for greater dose accuracy and minimum waste of precious drugs.

1.1 Selection of polymers for pharmaceutical packaging and delivery systems

Polymeric materials in contact with a drug product should fulfil a number of requirements besides the typical requirements like adequate mechanical properties and suitability for mass production. The polymer should be chemically resistant towards the excipients of the drug product. Moreover, it should be suitable for sterilisation, have good barrier properties towards water, preservatives and preferably also gases. It should comply with the existing regulations regarding the amount and toxicity of leachables. The number of commercially available polymer materials which can be used is rather limited. Moreover, the polymeric materials are typically hydrophobic, which is known to be a disadvantage with respect to protein adsorption.

In the field of diabetes treatment, compatibility of the polymer materials with insulin is extremely important. Compatibility between a polymer and insulin covers for instance good chemical and physical stability of insulin, low level of non-toxic leachables, and inhibition of insulin adsorption. In order to simplify the studies in this thesis leachables analysis has been omitted. Surface characteristics are known to influence the amount of adsorbed protein per unit surface area, the adsorption kinetics,[1,2] and the rate of fibrillation.[3,4] It has been proposed that the insulin monomer would undergo conformational changes upon adsorption to a hydrophobic surface and may thereby possibly initiate a fibrillation process.[5-8] The following mechanism has been proposed: Monomeric insulin is partially unfolded upon adsorption and can either refold to the native state or combine with other unfolded monomers. Nucleation is initiated and intermediate aggregates are formed. The intermediates can either fall apart or interact with unfolded species. When the intermediates reach a sufficient size, the surface area is large enough to stabilize the structure and combination with native molecules occurs. The slow formation of stable intermediates explains the lag phase which is often observed in insulin fibrillation experiments.[5,7] Furthermore, it has been indicated that the monomers have a higher tendency to adsorb to hydrophobic surfaces than the dimers and hexamers as the hydrophobic surfaces of the monomers are shielded when dimers or hexamers are formed.[5] Based on studies with hydrophilized chromium and titanium surfaces it seems like insulin dimers and hexamers are present at the hydrophilic surface and probably electrostatically bound to the surface. The studies also include a monomeric

insulin which does not adsorb to the hydrophilic surfaces.[9,10] The insulin analogue, insulin aspart (Asp^{B28} insulin) in the thesis is characterized by a significantly reduced tendency to form dimers and hexamers. Asp^{B28} insulin was also chosen as it is of interest for e.g. continuous subcutaneous infusion and promising results in simulated use in infusion pumps have been reported.[11]

1.2 Scope

The aim of the PhD project was to modify commercially available thermoplastic materials with a polymeric material in order to expand the utilisation of the polymers for pharmaceutical packaging and delivery systems. The primary goal was to improve the compatibility with insulin which was assessed by evaluating the chemical and physical stability of insulin as well as the ability to prevent adsorption of insulin. Secondary, long-term stability of insulin and thus the polymeric materials was important for the applications. Therefore, accelerated insulin stability studies at elevated temperatures as well as real-time studies were conducted. Moreover, only synthesis procedures which will result in firmly anchored polymeric layer should be considered. Surface-Initiated Atom Transfer Radical Polymerization (SI-ATRP) was chosen to prepare hydrophilic grafts *from* the thermoplastic materials. In addition to the covalent bond to the surface, the method offered versatility in selection of monomers, low polymerization temperatures, aqueous or methanolic media, and the possibility to obtain well-defined structures.

1.3 Thesis outline

The thesis briefly introduces the requirements and the characteristics of the polymer materials, which is needed to inhibit protein adsorption (*Chapter 2*). The techniques available for surface modification of organic/polymeric substrates are compared in *Chapter 3*. SI-ATRP was selected to graft hydrophilic polymers *from* polymeric substrates. *Chapter 4* introduces SI-ATRP and how initiating sites can be prepared on organic/polymeric substrates. Moreover, two relatively new catalytical methods, activators generated by electron transfer (AGET) and activator regenerated by electron transfer (ARGET) are outlined in which lower amount of catalyst is used in combination with a reducing agent. Many of the coatings prepared by SI-ATRP have been used for biological applications and proven to have a certain biofunctionality. Most of SI-ATRP studies in literature with proven biofunctionality for the grafts have been made on inorganic/metallic substrates; therefore, all types of surfaces combined with the applied monomers will be shown in *Chapter 5*. However, the literature survey in *Chapter 5* is only on biofunctional coatings which inhibit non-specific fouling. The other biofunctionalitites which include immobilization of biomolecules, adsorbents for proteins or cells, antibacterial activity, and encapsulation of

drugs can be found in the review article *Appendix A*. The characterization methods available for grafting *from* organic/polymeric substrates are very limited compared with inorganic/metallic substrates. The problem is highlighted along with a list of available techniques in *Chapter 6*. Initially, a model system consisting of surface functionalized poly(ether ether ketone) (PEEK) was applied. The hydrophilized PEEK had two applications, protein repellence and metallisation. Only the expected ability to repel proteins will be discussed in *Chapter 7*. The article in *Appendix B* contains both applications of the modified PEEK. Two stability studies were conducted with unmodified and modified polypropylene (PP) plates immersed in insulin. In the first study PP plates were modified with two types of hydrophilic grafts prepared by SI-ATRP. The second study was displaced 10 months from the first study; therefore, it was decided to implement experience from the first study and lower the amount of catalyst. Three different monomers were applied for ARGET SI-ATRP from PP in the second study. The results from two of them are included in *Chapter 8* whereas the work with the third is confidential and filed July 15th 2009 in a patent application, PCT Application No. PCT/DK2010/050187. *Chapter 8* also contains results from the first stability study and investigations with confocal fluorescence microscopy of insulin rejection or adsorption on modified and unmodified PP plates. The experimental work from the modification of PEEK and the work carried out in the first stability study are described in the articles *Appendix B-D*. The experimental procedures from the second stability study are outlined in *Chapter 8*. The surface modifications and most of the polymer characterization were made at the Danish Polymer Centre, DTU. Atomic force microscope analysis and X-ray Photoelectron Spectroscopy (XPS) were performed by employees at Risø DTU. High Performance Liquid Chromatography (HPLC) analysis was carried out in close collaboration with two technicians at Novo Nordisk A/S in Hillerød. The Thioflavin T (ThT) test was performed at Novo Nordisk A/S in Måløv. Metal analysis by Inductive Coupled Plasma Optical Emission Spectroscopy (ICP-OES) was made by Team Leachables & Metals from Chemistry Manufacturing Control Analytical Support at Novo Nordisk A/S. The adsorption studies with labelled insulin were carried out in close collaboration with the microscopy group at FeF Chemicals A/S. The microscopy group also supplied all the images from the Scanning Electron Microscope (SEM) analyses.

Appendix A. C.J. Fristrup, K. Jankova, and S. Hvilsted, Surface-initiated atom transfer radical polymerization – a technique to develop biofunctional coatings, Soft Matter, 5 (2009) 4623-4634.

Appendix B. C.J. Fristrup, K. Jankova, and S. Hvilsted, Hydrophilization of poly(ether ether ketone) films by surface-initiated atom transfer radical polymerization, Polym. Chem., 1 (2010) 1696-1701.

Appendix C. C.J. Fristrup, K. Jankova, R. Eskimergen, J.T. Bukrinsky, and S. Hvilsted, Protein repellent hydrophilic grafts prepared by surface-initiated atom transfer radical polymerization from polypropylene, submitted to Biomacromolecules.

Appendix D. C.J. Fristrup, K. Jankova, R. Eskimergen, J.T. Bukrinsky, and S. Hvilsted, Stability of Asp^{B28} insulin exposed to modified and unmodified polypropylene, submitted to Eur. J. Pharm. Sci.

2 Polymer and drug compatibility

The definition of compatibility from McGraw-Hill Encyclopedia of Science & Technology Online is as follows:

"The ability of two or more materials, substances, or chemicals to be used together without ill effect"

Control of the interactions between the polymer and the drug product formulation (in this case a protein formulation) is needed in order to obtain the compatibility. One way to attain compatibility is to reduce the extent of protein adsorption. Different approaches can be chosen to minimize protein adsorption. One method is passivation with sacrificial cheap proteins which are adsorbed at the surface in order to avoid adsorption of other proteins. A second method, which often is not feasible, is to stabilize the formation of the hydrophobic core of the protein by e.g. disulfide bonds. Finally, the approach from this project is stabilization of hydration at the surface by a hydrophilic coating.

2.1 Protein rejection or adsorption

Folding of proteins is controlled by non-covalent interactions like electrostatic, hydrogen bonding, van der Waals, hydrophobic, and acid/base. The same type of interactions controls the protein and surface interactions. The process involved in protein rejection or adsorption is energy-driven as well as dynamic and it can be described by the change in Gibbs free energy, ΔG.

$$\Delta G = \Delta H - T \cdot \Delta S$$

If ΔG is positive a repulsive force is present between the surface and the liquid protein layer. On the other hand, a negative ΔG will generate an attractive force which will result in protein adsorption. When an aqueous protein solution is exposed to a hydrophobic surface dehydration (release of water) occurs and the change in Gibbs free energy becomes negative as the entropy, ΔS increases.[12] Moreover, hydrophobic forces between the surface and the hydrophobic core of the protein will give a negative gain in enthalpy, ΔH, and contribute to the negative ΔG. A protein adsorbed to the hydrophobic surface is likely to denature by unfolding of the protein. The unfolding i.e. rearrangements in the protein structure will increase the enthalpy; however, the enthalpy for the overall protein adsorption process is negative. To sum up protein adsorption at a hydrophobic surface is an energetically favourable and irreversible process.[13]
Repulsion of proteins at hydrophilic surfaces is also a minimum interfacial energy phenomenon. In theory protein adsorption is less likely to appear as the

interfacial energy with water approaches zero. Proteins close to a low interfacial energy surface should not be under greater influence from the surface than from the bulk solution.[12] However, all surfaces are to some extend hydrophobic compared to water itself. For that reason, all surfaces exhibit some adsorption and denaturation of proteins.[13] A poly(ethylene glycol) (PEG) coating in aqueous solution is one of those materials which is able to resist protein adsorption. Some possible explanations to what makes PEG so unique is outlined below.

2.2 PEG and PEG-like coatings

PEG and PEG-like coatings are known to be able to inhibit non-specific fouling. PEG is water soluble and hydrophilic that means the PEG-coated surface is in a liquid-like state. Therefore, the hydrophilic PEG coating will provide very little stimulus for protein adsorption to occur due to hydrophobic interactions between the protein and the surface. Moreover, attractive interactions like van der Waal forces are expected to be weak as the coating and protein layers are quite dilute.[14] PEG has a large excluded volume in water; therefore, repulsive forces are generated when the volume available for the PEG chains is reduced by the approaching protein (Figure 2.1A). The PEG chains also exhibit a high mobility in water (Figure 2.1B) and the mobility of PEG will increase with the chain length (up to 100 ethylene oxide (EO) units).[12]

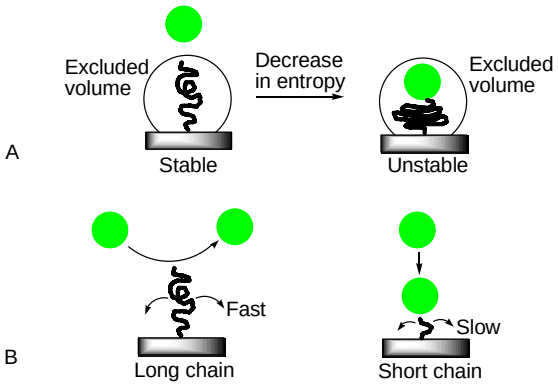

Figure 2.1 Mechanisms involved in rejection of proteins at PEG or PEG-like coatings. (A) The large excluded volume in water will lead to steric repulsion. (B) Long chains will have high mobility whereas short chains will have low mobility. Figure modified from Lee *et al.*[12]

The fast moving PEG chains will limit the time of residence at the surface for the proteins. Therefore, long PEG chains prevent protein adsorption more sufficiently than shorter chains.[12]

2.3 Characteristics of non-fouling coatings

A summery is presented of some of the most important characteristics and properties of non-fouling coatings which have been reported in literature. It will not be possible to obtain all of them as some of them are conflicting:

- Hydrophilic and highly hydrated
- Branched polymer architectures
- High grafting density
- Chain length
- Flexible
- Firmly anchored
- Uncharged surfaces → no electrostatic interactions
- Methoxy end groups rather than hydroxyl

Hydrophilicity and solubility in water have been mentioned before as essential properties of the polymer coating. The architecture of the polymer coating is very crucial for the ability to suppress non-specific fouling. A branched polymer architecture (Figure 2.2A) is one feasible structure for a non-fouling coating. Another possibility is a high grafting density which means that the polymer chains are attached close to each other (Figure 2.2B). A study with star shaped PEG and linear PEG has shown excellent repulsion of both insulin and lysozyme when the PEG coating had a high surface coverage (branched structure or high grafting density). However, a coating with longer PEG chains resulted in a lower grafting density (Figure 2.2C) which only inhibited adsorption of the larger lysozyme and not of the smaller insulin.[15]

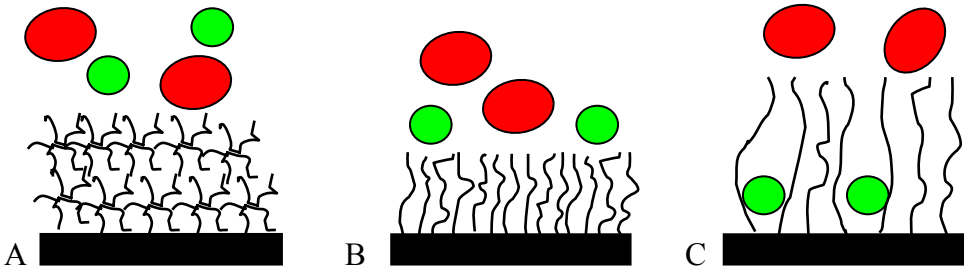

Figure 2.2 A branched polymer coating (A) and a polymer coating with high grafting density (B) will inhibit non-specific fouling; if the grafting density is insufficient some fouling may occur (C); the red proteins are lysozyme and the green are insulin. Figure modified from Groll *et al.*[15]

Good non-fouling properties of coatings are often not only ascribed to the chain length. Most studies, which investigate the influence of the chain length, assume high enough grafting density. Prime and Whitesides[16] discovered that for physical adsorbed PEG coatings >2 EO units were sufficient to suppress fouling. Others have reported 35-100 EO units for different PEG-containing coatings in order to obtain efficient repulsion.[17-19] Flexibility of the polymer coating is related to the chain length of the polymer grafts and it will increase with the chain length. Moreover, bulky side groups will decrease the flexibility; especially, if they are incompatible with aqueous solutions as water will be hindered sterically. The coating should be firmly anchored to the surface to have prolonged stability. In case of adsorption of a coating instead of a covalent bonding interfacial exchange could happen, this is replacement

of the adsorbed polymer layer by protein. If uncharged coatings are applied protein adsorption due to electrostatic interactions can be avoided, regardless of the isoelectric point of the protein. Kato *et al.*[20] have investigated the influence of ionic surfaces on the tendency to repel or adsorb proteins. Ionic polymer grafts repelled proteins with the same charge sign and accelerated adsorption of proteins with the opposite sign. Finally, methoxy groups are found to be more stable than hydroxyl.[14] Difference in inhibition of non-specific fouling has not been reported when PEG coatings with free methoxy and hydroxyl end groups were compared.[16]

3 Surface modification

Polymer coatings on polymeric substrates can be prepared by various techniques and they can be covalently attached, physically adsorbed, or surface entrapped. Commercially available thermoplastics do not always contain functional groups which can be applied for anchoring of reactive groups or polymer grafts. Therefore, most covalently attached polymer coatings require an initial activation of the surface before the coating is prepared. Activation of inert polymeric substrates is often performed with methods like ultraviolet (UV) irradiation, gamma irradiation, corona discharge treatment, or plasma discharge. Different reactive species e.g. radicals or oxygenated species are formed; however, the chemistry on the surface is not well-characterized. Another strategy is to use a chemical reagent to activate the surface which will result in specific reactive groups on the surface. Examples of how to activate the surface of inert polymeric substrates are outlined in "Grafting *from* and grafting *onto*" (3.1.1) and "Surface-anchored initiators" (4.1).

3.1 How to apply a polymer coating to the surface

Three different methods are available to apply a PEG or PEG-like coating on a polymer surface that is grafting, physical adsorption, and surface entrapment. Grafting involves a coating which is covalently bonded to the surface. It can either be made by grafting *from* or grafting *onto*. Grafting *from* implies polymerization of polymer chains from the surface by adding monomers whereas grafting *onto* means covalently bonding of the polymer chains to the surface. Physical adsorption is another way to apply a PEG-like coating. However, the molecular weight of PEG homopolymers should be above 100,000 if they should adsorb to hydrophobic surfaces. It is more favourable to use PEG-containing block copolymers as they will be more stable than the homopolymers. Hydrophobic segments of the block copolymers provide adsorption forces to the hydrophobic polymer substrate.[12] The third technique, the surface entrapment consists of immersion of the PEG or PEG-like coating and the substrate in a mutual solvent.[21] Swelling will occur and the polymer network on the surface of the substrate will loosen. The polymer coating molecules will diffuse into the interface. At the end the system is quenched with water as it is not a solvent for the substrate.

The advantages and disadvantages of the three coating techniques are listed in Table 3.1. Coatings made by grafting will have a long-term stability; however, they can be very time-consuming to prepare as it involves synthesis. The two other methods are simple in comparison with grafting but they are presumable not as stable as the covalently bonded coating. The surface entrapment technique also has some additional disadvantages as the molecular

weight has influence on the solubility and it might be necessary to replace the solvent if the composition of the polymer coating is changed.

Table 3.1 Pros and cons of the different techniques to apply a coating to a polymer surface.

Method	Advantages	Disadvantages
Grafting	Permanent; long-term stability	Time-consuming
Physical adsorption	Simple method	Not permanent
Surface entrapment	Simple method	Limitations in molecular weight if sufficient entrapment should be obtained

The grafting technique was chosen as long-term stability was important for pharmaceutical packaging and delivery systems.

3.1.1 Grafting *from* or grafting *onto*

When polymer chains are grafted *onto* a surface it requires reactive functional groups on the surface in order to attach the polymer chains. For polymeric substrates different chemical coupling reactions are employed to perform grafting *onto*. The chosen coupling reaction depends on the reactive groups on the surface which may have to be formed prior to the grafting *onto*. Figure 3.1 shows an example of chemical coupling of PEG to poly(ethylene terephthalate) (PET). PET films were reacted with 50% aqueous ethylene diamine to form amide bonds and cause chain cleavage.[22] The resulting primary amines were used for coupling of cyanuric chloride activated PEG which was prepared as described by Shafer and Harris.[23]

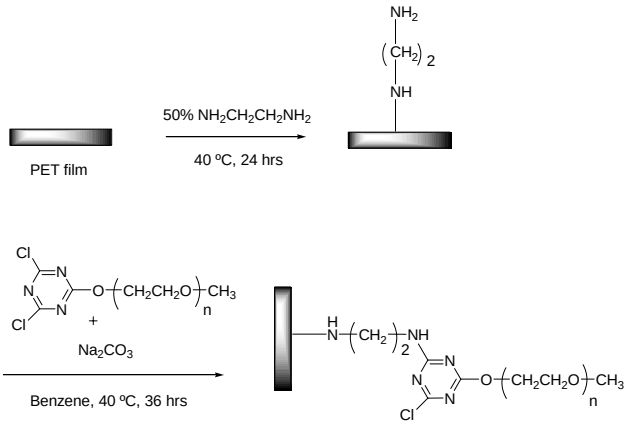

Figure 3.1 Coupling of cyanuric chloride activated PEG to PET films which have been treated with ethylene diamine.

Grafting *onto* has the advantage that the molecular weight of the polymer grafts can be determined before they are attached. However, steric hindrance of either the reactive groups on the surface or the polymer chains is expected to result in low grafting density.

Several graft polymerization techniques are available to prepare polymer chains which are grafted *from* the surface. Methods like plasma-induced or irradiation-induced graft polymerization have received a lot of attention in the biomedical research area. Treatment with plasma or irradiation has the advantage that inert materials can be activated using the same equipment. In Figure 3.2 poly(tetrafluoroethylene) PTFE films were hydrophilized by H_2 plasma treatment as polar and oxygenated species e.g. hydroperoxide and peroxide were formed after exposure to air. The monomer, poly(ethylene glycol)methyl ether methacrylate (MPEGMA) was physically adsorbed by solution coating which was followed by argon plasma-induced graft polymerization. The resulting plasma-polymerized MPEGMA (pp-MPEGMA) was covalently attached to the PTFE surface.[24]

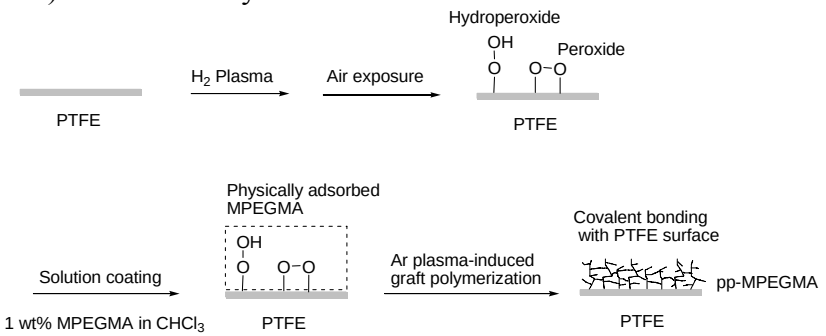

Figure 3.2 Argon plasma-induced graft polymerization of MPEGMA from H_2 plasma pretreated PTFE films.

A major drawback of plasma-induced or irradiation-induced graft polymerization is the large number of possible radical reactions which lead to an unknown chemical composition of the polymer coating. In order to overcome this problem as well as heating of the substrate pulsed plasma discharges have been introduced. Pulsed plasma polymerization is claimed to increase control of the coating chemistry which will result in less crosslinking.[25] However, the challenge with free radicals trapped within the polymer network will always be present for coatings prepared by plasma or irradiation polymerization. The free radicals often cause degradation as various aging processes are initiated in open atmosphere.[26]

In order to obtain good control over the polymers grafted *from* the surface another procedure must be followed. The thickness of the polymeric layer can be controlled and block copolymer brushes can be obtained with cationic and anionic graft polymerization. However, these methods are not used very often as formation of surface bound initiators is troublesome and only a few monomers can be applied. In contrast, conventional free radical polymerization (CFRP) has fewer restrictions but block copolymer brushes cannot be made. A thick polymeric layer can be prepared by CFRP. Moreover, the grafting density can be controlled by carefully choosing the right polymerization conditions as well as the initiator.[27] SI-ATRP combines the best from the two worlds; therefore, the versatility is great which makes it the most widespread method to graft *from* the surface. The chain length and the

grafting density have the potential of being controlled in SI-ATRP. Furthermore, SI-ATRP offers the possibility to obtain control of the polymer architecture and design linear or block shaped grafts. Several procedures are available to prepare initiating sites on polymeric/organic or metallic/inorganic substrates. Hydrophilic brushes can be prepared by SI-ATRP under mild polymerization conditions i.e. room temperature and in aqueous or methanolic media. The favourable polymerization conditions and the controllability, in particular make SI-ATRP of interest for this project.

4 Surface-Initiated Atom Transfer Radical Polymerization

Atom Transfer Radical Polymerization (ATRP) was introduced by Matyjaszewski[28] and Sawamoto[29] using different catalyst systems. Matyjaszewski also has a patent application on ATRP which was published in 1996.[30] ATRP is a controlled method which converts monomers to polymers by using radical polymerization (Figure 4.1). The initiators used for ATRP are commonly simple alkyl halides. A halogen atom X is transferred during the polymerization. Moreover, a catalyst system is present which consist of a transition metal complexed by one or more ligands. The catalyst provides equilibrium between the active form and the inactive form (called the dormant state). The equilibrium is displaced towards the dormant state; therefore, the polymer chains will only be active for a short time, thus allowing for a suppression of chain termination reactions and thereby controlling the polymerization. A controlled polymerization method like ATRP will result in narrow molecular weight distributions and controlled molar masses.

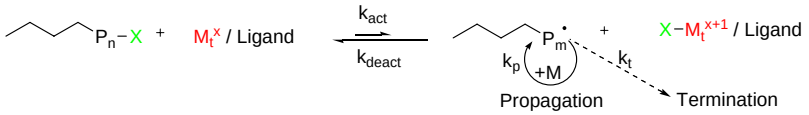

Figure 4.1 Scheme showing the principle of Atom Transfer Radical Polymerization.

When ATRP is performed from a surface it is called SI-ATRP. The initiating groups are attached to the surface; therefore, it is more sterically crowded, transport of the components is needed, and only the boundary layer is liquid. Consequently, the kinetics of SI-ATRP and ATRP are different and SI-ATRP is expected to take place with a lower reaction rate. Figure 4.2 shows that hydroxyl groups on the surface can be converted into initiating groups for SI-ATRP. After the polymerization the substrates are cleaned in order to remove the catalyst system and the residual monomer. The formed polymer grafts are covalently attached to the surface.

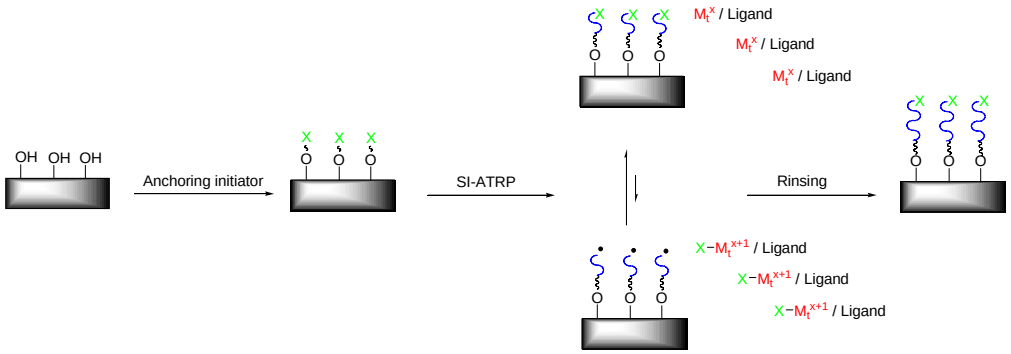

Figure 4.2 The principle of SI-ATRP; initially initiating groups are attached, then SI-ATRP is performed, and finally the catalyst system and the residual monomer are removed.

The anchoring of initiating groups is a very essential step and it depends on the surface of the substrate which does not always contain hydroxyl groups. Moreover, the initiating groups should be suitable for the particular monomer(s).

4.1 Surface-anchored initiators

Inherent initiating groups for SI-ATRP are present in a few synthetic polymers. Merrifield resins (with chloromethyl polystyrene)[31] as well as cross-linked[32,33] or not cross-linked[34] poly(4-vinylbenzyl chloride) (PVBC) can be used as received for SI-ATRP. Secondary fluorine atoms on the surface of poly(vinylidene fluoride) (PVDF) have also been claimed to act as initiators for the direct SI-ATRP of various monomers.[35,36] Other materials need immobilization of initiating sites on the surface prior to the SI-ATRP. The methods available to form surface-anchored initiators (SAIs) depend on whether the applied substrate is organic/polymeric or inorganic/metallic. Only the organic/polymeric substrates which have been modified with biofunctional coatings by SI-ATRP will be discussed. Preparation of SAIs on inorganic/metallic substrates is shown in the review article about biofunctional coatings.[37] Additionally, several recent reviews are dealing with SI-ATRP used as a tool for the modification of polymer materials,[38] cellulose,[39] silica nanoparticles,[40] carbon nanotubes[41] or various substrates.[42,43]

The polymeric substrates and their original functional groups are summarized in Figure 4.3. These functional groups can be transformed into initiating groups for SI-ATRP as explained below. Many natural materials are endowed with hydroxyl groups whereas amino groups on the surface occur more rarely like in chitosan. Cellulose membranes,[44] paper or NH_2-glass slides[45] were for example reacted with 2-bromoisobutyryl bromide (Br-*i*-BuBr) and triethylamine (TEA) to form the bromoester or bromoamide initiator. When Br-*i*-BuBr is used in a mixture with the inert propionyl bromide, surfaces having the whole range from 0 to 100% ATRP initiator functionality can be obtained.[45] The hydroxyl groups available on the surface of poly(hydroxyethyl methacrylate)-*co*-poly(methyl methacrylate) (PHEMA-*co*-PMMA)[46] hydrogels are reacted with Br-*i*-BuBr to create the activated bromide as surface initiator.

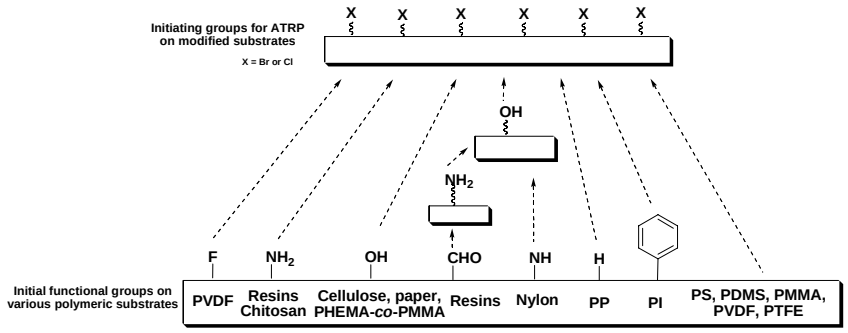

Figure 4.3 Preparation of initiating sites for SI-ATRP on organic/polymeric substrates.

If the surface does not contain any hydroxyls, attempts are made to form hydroxyl groups: The commercial matrix for Electrostatic Ion Chromatography columns, Toyopearl® AF-650M contains surface aldehyde groups. The aldehydes on the surface undergo a sequence of reactions via amino, ring-opening of δ-gluconolactone into hydroxyls, and finally into chloropropionate initiating sites.[47] Nylon membranes can be activated with formaldehyde.[48] Initiating sites for SI-ATRP were also successfully attached to inert PP surfaces (CH_2) by use of UV irradiation. Benzophenonyl 2-bromoisobutyrate (Figure 4.4) was synthesized from 4-hydroxybenzophenone and Br-*i*-BuBr, and was used as UV initiator. The formation of covalent C-C bonds was obtained by a procedure including spin coating of the UV initiator from a toluene solution onto PP surfaces, followed by UV treatment at λ = 365 nm.[49]

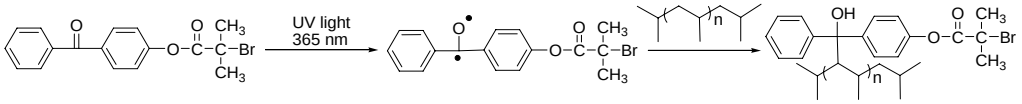

Figure 4.4 Formation of SAIs on PP by UV irradiation of benzophenonyl 2-bromoisobutyrate.

Other specific reactions on polymers to form the SAIs also exist. Polyimide (PI) films have been anchored with benzyl chloride initiating sites for SI-ATRP by chloromethylation with paraformaldehyde/Me_3SiCl in the presence of $SnCl_4$.[50] Ozone-pretreated PVDF has been thermally reacted with 2-(2-bromoisobutyryl)ethyl acrylate to prepare the SAIs.[51,52] Chemical vapor deposition polymerization of [2.2]-paracyclophane-4-methyl 2-bromoisobutyrate[53] (Figure 4.5) resulted in grafting (poly(dimethylsiloxane) (PDMS), PMMA, PTFE, and polystyrene (PS)) with initiating sites for SI-ATRP.

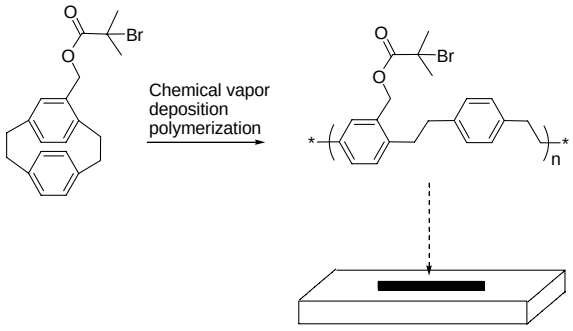

Figure 4.5 Initiating groups for SI-ATRP immobilized on various substrates by chemical vapor deposition polymerization of [2.2]-paracyclophane-4-methyl 2-bromoisobutyrate.

4.2 Lower amount of catalyst

For medical devices and pharmaceutical packaging the presence of copper from the catalyst can have an undesirable impact on the drug and as a

consequence the health of the patient. Therefore, methods which will lower the amount of catalyst are to be preferred. In a broader perspective lowering the amount of catalyst will be beneficial both commercially and environmentally. In order to minimize the amount of copper from the catalyst Matyjaszewski and coworkers have introduced two new catalytical methods in which Cu^{II} in combination with a reducing agent is used instead of Cu^{I}. Activators generated by electron transfer (AGET) SI-ATRP was first introduced which uses >1000 ppm catalyst and nearly stoichometric amounts of reducing agent. The most recent development is activator regenerated by electron transfer (ARGET) SI-ATRP. In ARGET SI-ATRP the amount of copper catalyst is significant lower (tens of ppm values vs. monomer) and a large excess of reducing agent is applied.[54,55] ARGET SI-ATRP differs from SI-ATRP in lower amount of catalyst and ligand and presence of reducing agent. Moreover, Cu^{II} is applied instead of Cu^{I} and continuously reduced by the reducing agent (Figure 4.6).

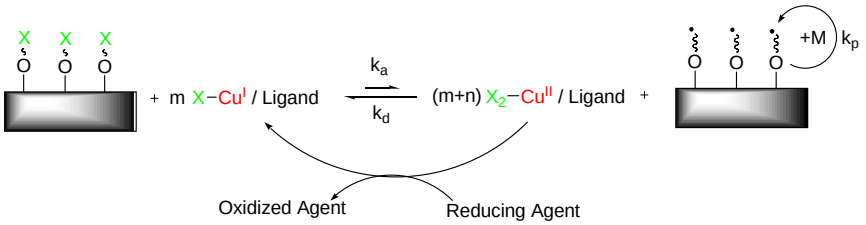

Figure 4.6 Principle of ARGET SI-ATRP; Cu^{II} is continuously reduced by the reducing agent to Cu^{I}.

Most studies with AGET and ARGET have been made in solution and not from surfaces; however, inspiration from these experiments can be used for SI-ATRP. AGET ATRP utilizes reducing agents which are unable to initiate new chains. The reducing agent reacts with the Cu^{II} complex and forms the Cu^{I} ATRP activator. Cu^{0}, Sn^{II} 2-ethylhexanoate, ascorbic acid, and triethylamine have been reported as reducing agents for AGET ATRP. In ARGET ATRP the Cu^{II} is continuously reduced to Cu^{I} as a large enough excess of reducing agent to copper is applied. This makes it possible to lower the concentration of catalyst to initiator significantly. Good control was obtained with 50 ppm of copper for ARGET ATRP of acrylate and 10 ppm of copper for styrene polymerization. In addition to the reducing agents for AGET ATRP a number of organic derivatives of hydrazine, phenol, sugar, and ascorbic acid as well as inorganic species such as Sn^{II} and Cu^{0} can be used for ARGET ATRP.[56] The AGET process is more sensitive to the added amount of reducing agent than ARGET. On one hand, a large excess of reducing agent in AGET will result in a large amount of Cu^{I} ATRP activator and as a consequence a fast uncontrolled process. On the other hand, an insufficient amount of reducing agent will not consume the air present and the polymerization will not occur. Removal of air from the system can especially be problematic for SI-ATRP from large substrates or large batches. Therefore, ARGET ATRP is more suitable for grafting *from* a surface than AGET.[57]

5 Biofunctional coatings

Various monomers have been used for SI-ATRP to prepare polymer coatings which can be applied within the field of biotechnology. The term biofunctionality is used to emphasize that the polymer coating is not only of interest in biological applications but also that it has been tested within these applications. The monomers in Table 5.1 have been used for SI-ATRP and the resulting polymers have been investigated with respect to their biofunctionality. However, some of the polymers are not homopolymers. This is indicated by the letter "a" for diblock copolymers, "b" for copolymers, and "c" for comb copolymers. Six classifications for biofunctionality have been chosen in order to elucidate the applications of the monomers. The classifications include inhibition of non-specific fouling, immobilization of biomolecules, separation of proteins, adsorbents for proteins or cells, antibacterial activity, and encapsulation of drugs. Only examples within inhibition of fouling will be discussed here whereas the other biofunctionalities are included in the review article.[37]

Table 5.1 Survey of polymer grafts with different biofunctionalities prepared by SI-ATRP and reported in the literature between 1997 and 2009. Biofunctionality: Inhibition of non-specific fouling (I), Immobilization of biomolecules (II), Separation of proteins (III), Adsorbents for proteins or cells (IV), Antibacterial activity (V), and Encapsulation of drugs (VI).

Monomer	Biofunctionality						Substrate	Catalyst:ligand	Solvent
	I	II	III	IV	V	VI			
AA				44			Cellulose	CuCl:Me_4Cyclam	Water
	58b						Stainless steel	Grubbs catalyst	Toluene
AAm			61,62				Silica	CuCl:Bipy	DMF
	59,60						Silicon	CuCl:Bipy, CuCl/$CuCl_2$:Bipy	DMF, water
*t*BA		63					Gold	CuBr:PMDETA	Acetone
*t*BAEMA	58,58b						Stainless steel	Grubbs catalyst	Toluene
*t*BMA				64			Silicon	CuBr:PMDETA	Toluene
CBMA	65,66	65					Gold	CuBr:Bipy	Methanol:water
DEAEMA						67b	Gold	CuBr:SP	DMF
DMAEMA	68			68		67b	Gold	CuBr:Bipy, CuBr:SP, CuBr/$CuBr_2$:HMTETA	Water, DMF, acetone
					45		Glass/filter paper	CuBr:Bipy	*o*-DCB
					49		PP	CuCl/$CuCl_2$:HMTETA	Acetone
					32		PVBC	CuCl/$CuBr_2$:Bipy	DMF
					52		PVDF	CuCl/$CuCl_2$:Bipy	Water
					40		Titanium	CuCl/$CuCl_2$:PMDETA[69]	DMF[69]
DMAAm			47				Toyopearl®	CuCl/$CuCl_2$/Cu powder:HMTETA	Water
GMA		71b					Fe_3O_4 NP	CuBr:PMDETA	Methanol
	70a,c	72		70			Silicon	CuCl/$CuCl_2$:Bipy	DMF:water
GMMA		71b					Fe_3O_4 NP	CuBr:PMDETA	Methanol
HEMA		74,75					Glass	CuCl/$CuBr_2$:Bipy	Water
		76-79					Gold	CuCl/$CuBr_2$:Bipy	Water
	48,48a						Nylon	CuBr/$CuBr_2$:HMTETA	Water
			82				Silica	CuBr:Bipy	Methanol
	60,73	75,80		73			Silicon	CuCl/$CuCl_2$ (Br_2):Bipy	Water
		81					Titanium	CuCl/$CuCl_2$:PMDETA	Water
MAAS	83	83					Titanium	CuCl/$CuCl_2$:PMDETA	Water
MAIpGlc	84						Silicon	CuBr:Me_6TREN	Veratrole
MEMA	60						Silicon	CuCl/$CuCl_2$:Bipy	Methanol
MMA				86			Diamond	CuCl/$CuCl_2$:PMDETA[87]	Toluene[87]
	85a						Fe_3O_4 NP	CuCl:Bipy	DMF
				60			Silicon	CuCl/$CuCl_2$:Bipy	THF
MPC	64,88-90						Silicon	CuBr:Bipy	Methanol, methanol:water
MPDSAH	91						Gold	CuBr/$CuBr_2$:Bipy	Methanol:water
MPEGMA	92						Glass	CuBr:Bipy	Methanol:water
	66,93-96	76,77,100				67b	Gold	CuBr:SP, CuCl/$CuBr_2$:Bipy, CuBr:Bipy	DMF, water, methanol:water
	46						Hydrogels	CuBr:Me_6TREN etc.	Water

Monomer	Biofunctionality I	II	III	IV	V	VI
MPEGMA	35,36					
	97					
	93,97	101,102b				
	92					
	58,98					
	98,99					
	53					
NIPAAm	103			103		
		106				
						110
	34					
			107-109			
	70,104,105,105a,b					111
PEGMA	85a,112					
	113	74,75				
	114,115	114		115		
	48,48a					
	116					
	51					
	105,105a,b,113,11 4,117	75,101b,114,117				
SBMA	66,94,118,119					
Sodium acrylate		120				
SPM					94	
			121			
Styrene				86		
				58,58b		
				60		
2-VP				122		
4-VP					50	
					33	

Substrate	Catalyst:ligand	Solvent
PVDF	CuCl/$CuCl_2$:Bipy, CuCl:DMDP	Water, NMP
Silica	CuCl/$CuCl_2$:Bipy	Methanol
Silicon	CuCl (Br)/$CuCl_2$ (Br_2):Bipy, CuBr:PMDETA	Methanol, water, ethanol
Silicon oxide	CuBr:Bipy	Methanol:water
Stainless steel	Grubbs catalyst, CuBr:PMDETA	Toluene, water
Titanium	CuBr:PMDETA	Water
Various	CuBr/$CuBr_2$:Bipy	Water
Gold	CuBr:Bipy	Water
Magnetic NP	CuCl:Bipy	DMSO
MCF	CuBr:PMDETA	Ethanol
PS	CuCl/$CuCl_2$:Me_6TREN	Water
Silica	CuCl/$CuCl_2$:Me_6TREN, CuCl:Me_6TREN	Water/2-propanol, DMF
Silicon	CuCl (Br)/$CuCl_2$ (Br_2):HMTETA, CuCl/$CuCl_2$:Bipy, CuBr:PMDETA	DMSO, methanol:water
Fe_3O_4 NP	CuCl:Bipy	Water, DMF
Glass	CuBr/$CuBr_2$:Bipy, CuCl/$CuBr_2$:Bipy	Methanol:water
Gold	CuCl/$CuCl_2$:Bipy, CuBr:Bipy	Water, methanol:water
Nylon	CuBr/$CuBr_2$:HMTETA	Water
PI	CuCl/$CuCl_2$:Bipy	Water, DMF:water
PVDF	CuCl/$CuCl_2$:Bipy	Water
Silicon	CuBr/$CuBr_2$:HMTETA, CuCl (Br)/$CuCl_2$ (Br_2): Bipy	DMSO, water, methanol:water
Gold	CuBr:Bipy, CuBr/$CuBr_2$:Bipy	Methanol:water
Silicon	CuBr/$CuBr_2$:Bipy	-
Gold/silicon	CuCl/$CuCl_2$:Bipy	Methanol:water
PS seed latex	CuCl/$CuCl_2$:Bipy	DMF:water
Diamond	CuBr:Bipy	-
Stainless steel	Grubbs catalyst	Toluene
Silicon	CuCl/$CuCl_2$:Bipy	THF
Gold	CuBr/$CuCl_2$:Me_6TREN	Acetonitrile
PI	CuCl/$CuCl_2$:Me_6TREN	2-Propanol
PVBC	CuBr/$CuBr_2$:Me_6TREN	2-Propanol

a Diblock Copolymer

b Copolymer

c Comb copolymer

5.1 Inhibition of non-specific fouling

Inhibition of non-specific fouling, non-fouling, antifouling, and resistance against biofouling are terms to describe surfaces which reduce both protein adsorption and cell adhesion. Interactions between the proteins or cells and the surface determine the tendency to undergo non-specific fouling. Hydrophobic and electrostatic interactions are considered to be the major driving forces for fouling; but the importance of these interactions depends on the protein structure and the surface properties. For instance, non-specific fouling depends on the surface wettability, specific chemical groups on the surface, surface charge, the balance between hydrophobic and hydrophilic groups, the mobility of the polymer brushes, and the structure of the adsorbed water.[97]

5.1.1 General examples of non-fouling polymeric grafts

In Table 5.1, MPEGMA and poly(ethylene glycol) methacrylate (PEGMA) appear to be the most frequently used monomers to prepare non-fouling surfaces by SI-ATRP. PEG and its derivatives are finding more and more biological applications as PEG is known to prevent protein adsorption, to suppress platelet adhesion, and to reduce cell attachment and growth.[117] Stainless steel and titanium are applied in medical devices due to their high strength, corrosion resistance, and biocompatibility. In order to prevent non-specific fouling on the metal, poly(MPEGMA) was grafted from the substrate.[98] Many studies have been made to investigate the influence of graft density and chain length on the inhibition of non-specific fouling. One study with MPEGMA has looked at the influence of the MPEG chain length on short- and long-term fouling resistance of the polymer coatings. MPEGMA's with side chains of 4, 9, and 23 EO units were included in the study. The short-term results for the three poly(MPEGMA)'s grafted from titanium showed reduced cell adhesion for three weeks compared to bare titanium. When the samples were kept for a longer time, they were completely covered with cells in 7, 10, and 11 weeks for poly(MPEGMA) with 4, 9, and 23 EO units respectively.[99] Another study with grafted brushes of poly(MPEGMA) from poly(HEMA-*co*-MMA) hydrogels showed increasing cell repellency with increasing chain length compared to the untreated hydrogels.[46] Singh *et al.* proved that the transition from mushroom to brush regime affects both the peptide adsorption and the cell adhesion. Peptide adsorption and cell adhesion occurred only in the mushroom regime for poly(PEGMA) grafted from gold. In the brush regime, when the graft density was high, there was negligible peptide adsorption and cell adhesion. Moreover, peptide adsorption in the mushroom regime promoted cell adhesion on the substrates, in contrast to the brush regime where cell adhesion was resisted even after preadsorption of an adhesion-promoting peptide.[115] Many claim that the graft density is the most important parameter with respect to non-fouling properties of grafted polymers prepared by SI-ATRP and that the chain length or molecular weight

of the polymer grafts has a weaker influence.[115] Feng *et al.*[89] have verified this observation with poly(2-methacryloyloxyethyl phosphorylcholine) (poly(MPC)) grafted surfaces in some fibrinogen adsorption experiments in which the graft density was varied from 0.06 to 0.39 chains/nm^2 and the chain length was from 5 to 200 MPC units. On the other hand, too high a graft density may cause detachment of the polymer brushes. Experiments with PEGMA polymerized from silicon or glass have shown that when a solution with only ATRP initiator modified trimethoxysilane was replaced by a mixture of 60 mol% ATRP initiator modified trimethoxysilane and 40 mol% inert trimethoxysilane, the stability of the poly(PEGMA) was enhanced from 1 to more than 7 days without any reduction in the non-fouling properties.[113] Other monomers which have been shown to be capable of preventing non-specific fouling as homopolymers are acrylamide (AAm), 2-(*tert*-butylamino)ethyl methacrylate (*t*BAEMA), 2-carboxy-*N*,*N*-dimethyl-*N*-(2'-methacryloyloxyethyl)ethanaminium inner salt (CBMA), 2-(diethylamino)ethyl methacrylate (DMAEMA), HEMA, methacrylic acid sodium salt (MAAS), 3-*O*-methacryloyl-1,2:5,6-di-*O*-isopropylidene-D-glucofuranose (MAIpGlc), 2-methoxyethyl methacrylate (MEMA), MPC, (3-(methacryloylamino)propyl)-dimethyl(3-sulfopropyl) ammonium hydroxide (MPDSAH), *N*-isopropylacrylamide (NIPAAm), and sulfobetaine methacrylate (SBMA) (Figure 5.1A). The idea of incorporating phosphorylcholine moieties into the polymer coating originates from the fact that zwitterionic phospholipids, which are known from the outer membranes of cells, have been shown to be non-thrombogenic.[88] The monomers CBMA,[65,66] SBMA,[66,94,118,119] and MPDSAH[91] are zwitterionic like MPC. They were developed because the long-term stability of MPC is poor due to the tendency for MPC to undergo hydrolysis of the phosphoester group. Another reason for seeking other suitable monomers is the lack of stability of monomers containing PEG with hydroxyl end-groups, as they can be oxidized enzymatically to aldehydes and acids allowing proteins and cells to attach. Therefore, the utility of PEG and PEG derivates for applications which require long-term stability is reduced.[94] In addition, hydroxyl groups in e.g. PEG, PEGMA, and HEMA may form hydrogen bonds with proteins, thus allowing them to attach. This will decrease the long-term durability of the polymer grafts. Cho *et al.*[91] have published the first article on the non-specific fouling property of poly(MPDSAH)-coated surfaces. The poly(MPDSAH) brushes were able to suppress non-specific fouling to a level comparable to that of PEG-like coatings. The protein repellency was much better than that of phophorylcholine-based polymer grafts. Lysozyme, fibrinogen, bovine serum albumin (BSA), and ribonuclease A have been used as model proteins and the adsorption of proteins was < 0.6 ng/cm^2.[91] Homopolymer grafts of either poly(SBMA) or poly(AAm) were also able to inhibit bacterial adhesion in a flow chamber.[59,94] In order to prevent fouling, the optimum thickness for poly(SBMA) grafts was 62 nm in 100% blood serum and plasma. Yang *et al.*[119] also found that fouling decreased with increasing ionic strength. A study

which compared poly(CBMA), poly(MPEGMA), and poly(SBMA) grafts with self-assembled monolayers on gold showed higher resistance to fouling from 100% plasma for the polymer grafts. Poly(CBMA) was the most interesting polymer for blood-contacting applications, as it had the overall lowest level of protein adsorption and an anticoagulant activity was observed.[66] The monomer MAIpGlc can also be used to prepare blood-compatible polymer brushes. After SI-ATRP of MAIpGlc, deprotection and then sulfonation was performed. The resulting polymer brushes contained sulfonated sugar repeating units and they were claimed to mimic heparin. Heparin can participate in a catalytic cycle of coagulation factor inactivation. Moreover, it is known to reduce platelet adhesion and protein adsorption.[84]

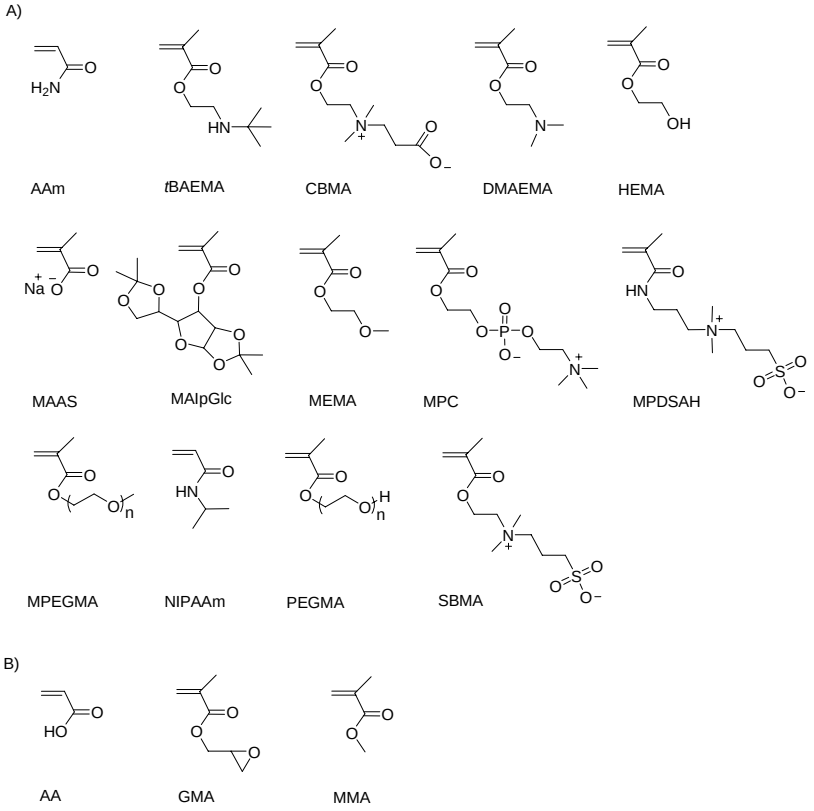

Figure 5.1 A) Polymer grafts on surfaces made from the monomers inhibit non-specific fouling; B) The monomers result in antifouling coatings when incorporated in copolymer structures.

HEMA[48] and MEMA[60] are similar to PEGMA and MPEGMA respectively, but they have a side chain containing only one EO unit. Poly(HEMA) showed the same correlation between graft density and cell/protein rejection as the poly(PEGMA) (*vide supra*).[73] Cationic poly(DMAEMA) brushes distinguish themselves by rejecting net positively charged lysozyme proteins and they have a high binding capacity for net negatively charged BSA.[68] Poly(NIPAAm) has been used to prepare thermoresponsive surfaces due to its lower critical solution temperature

(LCST) at about 32 ºC in aqueous solution. Below the LCST, poly(NIPAAm) is hydrophilic in water and cells can detach from the surface. If the temperature is increased to above the LCST, hydrogen bonding between the isopropylamide moiety and water molecules is lost and the surface becomes hydrophobic. Various cells will therefore adhere, spread and proliferate at 37 ºC on poly(NIPAAm) surfaces.[70,103,105] Li *et al.*[104] have also shown that, at 37 ºC and with a poly(NIPAAm) thickness of ≤ 45 nm, cells could adhere and proliferate. Above 45 nm, the cells could not adhere, whereas between 20 and 45 nm they could be attached or detached by switching the temperature.[104] Mizutani *et al.*[34] also demonstrated that the thicker the poly(NIPAAm) layer was the smaller was the amount of proteins adsorbed and cells adhered. For thin poly(NIPAAm) layers, the temperature had an impact, as cells detached at lower temperature (20 ºC).[34] Copolymer brushes with PEGMA[105] and comb copolymer brushes with glycidyl methacrylate (GMA)[70] (Figure 5.1B) have resulted in more rapid cell detachment during the temperature transition and cell recovery at 20 ºC, without influencing either cell adhesion or growth.

Ignatova *et al.*[58] have studied fouling on polymer coatings prepared from *t*BAEMA and mixtures of this monomer with acrylic acid (AA), MPEGMA, and styrene. Copolymer brushes of *t*BAEMA and AA or MPEGMA were more effective in avoiding protein adsorption than poly(*t*BAEMA) copolymers with styrene, and PS, whereas both homopolymer brushes of *t*BAEMA and copolymer brushes with MPEGMA and AA were more effective in decreasing bacterial adhesion than PS and copolymer brushes of *t*BAEMA and styrene.[58]

5.1.2 Non-fouling grafts for separation of proteins

SI-ATRP is a suitable method to modify column material for various chromatographic techniques in order to prevent protein adsorption to the packing material which is known to undermine purification, recovery, and analysis.[62] The polymer coating must be uniform to avoid blocking of the pores; moreover, it should be covalently attached to the surface, as polymers formed in solution inside the pores will block the pores. SI-ATRP also offers the ability to control the thickness of the polymer coating as opposed to conventional radical polymerization.[62] If the purpose is to separate proteins by chromatography, e.g. Size Exclusion Chromatography (SEC), Capillary Electrophoresis or High Performance Liquid Chromatography (HPLC), the column material could be modified with polymer brushes made from the monomers AAm,[62,66] *N*,*N*-dimethylacrylamide (DMAAm),[47] HEMA,[82] NIPAAm,[108] or SPM[121] (Figure 5.2).

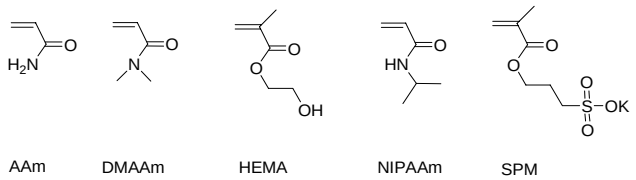

Figure 5.2 SI-ATRP of the monomers on column materials improves separation of proteins.

The grafting density and the chain length of the polymer brushes will influence the separation of proteins. With a high grafting density of poly(DMAAm), i.e. in the brush regime, separation of lower molecular weight proteins is possible. In the mushroom regime, i.e. at low grafting density, the proteins which can be separated include the high molecular weight proteins (> 100 kDa).[47] When the molecular weight of the poly(DMAAm) brushes is high, the separation of proteins with a large difference in molecular weight will be significantly better than with lower molecular weight brushes.[47] Studies with poly(NIPAAm) brushes have shown that separation of hydrophilic substances like proteins or peptides takes place only above the LCST transition. Therefore, proteins are separated through hydrophobic interactions whereas lower molecular weight substances are separated in the SEC mode. Thus, longer retention times are observed for hydrophobic steroids due to their longer permeation path through the matrix. For this reason, not only temperature but also the grafting density of poly(NIPAAm) is crucial for the elution of steroids due to the interactions between analytes and brushes and the dehydration of the poly(NIPAAm) brushes on the densely packed surface.[107-109]

6 Characterization methods

The biofunctional coatings prepared by SI-ATRP also need to be characterized in order to confirm e.g. formation of the initiating groups, determine the molecular weight of the polymer brushes or the grafting density, and evaluate the biofunctionality.

6.1 Characterization of polymer grafts

More methods are available when the initiating groups or polymer grafts are present on inorganic or metallic substrates compared with polymeric substrates as differences in refractive index and elemental composition can be utilized. For a polymeric substrate the lack of difference between the substrate and the SAIs or the polymer grafts make the characterization much more challenging. The characterization methods used in recent years are listed in Table 6.1. Especially, the SAIs on a polymer surface can be difficult to quantify with the techniques available. The brackets indicate that the technique might be used for some systems but it is not applicable for all materials within the group.

Table 6.1 Characterization methods used for SAIs and/or polymer grafts on organic/polymeric and inorganic/metallic substrates.

Techniques	Organic/polymeric		Inorganic/metallic	
	SAIs	Polymer grafts	SAIs	Polymer grafts
AFM		x	x	x
ATR-FTIR	(x)	x	x	x
DSC		(x)		x
Elemental analysis		(x)	x	x
Ellipsometry		(x)	x	x
Grazing angle FTIR			x	x
SEM		x	x	x
TEM			x	x
TGA		(x)	x	x
UV-VIS			(x)	(x)
WCA	x	x	x	x
XPS	x	x	x	x

For polymeric substrates X-ray Photoelectron Spectroscopy (XPS) is the predominant technique to confirm the presence of initiating groups on the surface.[34,48,50,53,116] Alternatively, characterization of the polymer grafts is used as an indirect proof for the formation of the initiating groups. The techniques to characterize the polymer grafts typically include e.g. Attenuated Total Reflectance (ATR) Fourier Transform Infrared (FTIR) spectroscopy,[34,44,49] water contact angle (WCA) measurements,[34,49] Scanning Electron Microscope (SEM) analysis,[48] XPS,[34,48,50,53,116] and Atomic Force Microscopy (AFM).[53] The thickness of the dry polymer grafts can be measured by ellipsometry.[34] Since none of the techniques have proven to be

very useful for quantification of the initiating sites it is also not possible to obtain information about the grafting density.

The list of characterization methods for inorganic or metallic substrates is more comprehensive as the differences between the organic layer and the substrate gives additional possibilities. As a consequence, more results with inorganic or metallic substrates have been published. The formation of initiating groups on inorganic or metallic substrates is often confirmed by FTIR[46,110,111] or FTIR equipped with a grazing angle accessories[91,100,114,115] as well as water contact angle measurements,[64,91,100,115] and XPS.[46,53,59,64,83-85,100-102,114] Other methods such as ellipsometry,[100] elemental analysis,[108,109] and AFM[64,102] are also applied to evaluate the presence of the initiating groups. Thermal Gravimetric Analysis (TGA),[110] Transmission Electron Microscopy (TEM) images,[77,110] and UV-visible spectroscopy[77] are methods that have been used more rarely; however, they can be very useful in some applications. The characterization methods for polymer grafts from inorganic or metallic substrates include many of the same techniques as for the initiating groups e.g. FTIR,[59,60,85,94,97,110,111] FTIR with grazing angle,[53,73,91,100,114] WCA,[46,60,64,83,91,100,104,111,113,115,120] and XPS.[53,59,81,83-85,94,101,102,104,114] In addition to the confirmation of the polymer coating prepared by SI-ATRP techniques like XPS,[75,91] ellipsometry,[44,53,59,64,78,79,94,104,113,114,120] and AFM[119,120] can also be applied to measure the thickness of the polymer grafts. Ellipsometry has even been used to determine the grafting density of polymer brushes.[115] Other interesting characteristics for the polymer grafts can also be evaluated e.g. surface topography by AFM,[59,64,101,102,104,120] weight loss by TGA,[85,97,110] temperature transition by Differential Scanning Calorimetry,[110] or calculation of the amount of various chemical elements by elemental analysis.[108,109] SEM[46,102,108] or TEM[77,85,110] images can give a visual confirmation of the polymers grafted from the substrate.

The molecular weight and the polydispersity index (PDI) of the polymers grafted from a substrate can be determined by two different approaches. The polymer chains can be cleaved from the substrate by etching with HCl[123] or HF[60,108,109,111] as well as by hydrolysis with NaOH.[47] This approach has been reported mainly for inorganic or metallic substrates whereas the other approach with a free or "sacrificial" initiator also has been used for polymeric substrates.[49,59,64,68,82] When adding a free or "sacrificial" initiator e.g. ethyl 2-bromoisobutyrate to the reaction mixture the amount of initiating groups on the substrate is neglected. Therefore, the molecular weight of the resulting bulk and grafted polymer is claimed only to be a function of the "sacrificial" initiator-to-monomer ratio.[124,125] Others even insist that addition of a comparatively large amount of "sacrificial" initiator to the polymerization is required to maintain adequate control of the SI-ATRP process.[126,127] Independent of the approach chosen the molecular weight and the PDI is determined by SEC. Moreover, the results from SEC analysis enable calculation of the grafting density.

6.2 Methods to demonstrate inhibition of fouling

Techniques to determine protein adsorption and cell attachment are of great interest to many researchers. The most common characterization methods to investigate non-spedific fouling are Surface Plasmon Resonance (SPR)[66,68,78,82,91,100,114,115,118,119] and Quartz Crystal Microbalance (QCM)[114] which both have a detection limit of 1 μg/cm^2. SPR and QCM are complementary methods to investigate binding characteristics of proteins or cells.[114] Both techniques are using specific substrates. For SPR substrates like gold, silver and copper can be applied. The surfaces can be modified with polymer grafts; however, the SPR biosensor has some limitations in the thickness of the polymeric layer. The polymer coating should be able to allow the light to go through as the incoming light induces formation of surface plasmon waves at the metal surface. The plasmons are sensitive to the refractive index at the boundary layer. When non-specific adsorption occurs the refractive index at the surface changes. The SPR detector monitors the changes in refractive index which allows us to follow adsorption in real time and measure changes in thickness.[128] The measurements with SPR may differ from the scope of the application as they are performed in a flow cell. The quartz crystal used for QCM has a layer of gold and electrodes plated on it. Moreover, the crystal is piezoelectric and mechanical deformation of the material is induced by an external electrical field.[129] A resonant oscillation should be obtained for the crystal close to the fundamental frequency of the crystal, and when non-specific adsorption takes place the frequency changes. The change in resonant frequency is measured and the mass of the adsorbed layer can be calculated. The application of the material should be considered before the QCM measurements are carried out as the possibilities are many among the commercially available systems. The measurements can be made in either static or flow sample cells under vacuum, in gas phase or in liquid environment.[130]

Fluorescence microscopy is a visual way to demonstrate non-specific adsorption of proteins[46,102,120] and cells or bacteria[81-83,113,118] and it relies on the use of fluorophores which will provide an image contrast. Synonyms for fluorophores are dyes, stains or labels. The fluorophore is either naturally present in the sample or added prior to the analysis. If the sample fluoresces by itself after absorption of light the process is called autofluorescence. Traditionally, wide-field fluorescence microscopes are applied to visualize non-specific fouling. However, the confocal fluorescence microscope will offer better resolution and the possibility of true three-dimensional optical resolution. A pinhole in front of the detector is used in a confocal fluorescence microscope to block the light from the out-of-focus planes. Fluorescence from the fluorophores in the out-of-focus planes causes blurring of the image in wide-field microscopy.[131]

7 Model system

Poly(ether ether ketone) (PEEK) has been applied as a model substrate for SI-ATRP. The substrates of interest were e.g. PP, polycarbonate, and cyclic olefin copolymers which are quite inert polymer materials; therefore, anchoring of initiating sites could be challenging. The aim of the experiments with the model system was to demonstrate that SI-ATRP of selected monomers could be performed and would result in hydrophilization of the substrate. The example below is with PEGMA grafted *from* PEEK by SI-ATRP. During the last 30 years PEEK has been known for its biological applications which require surface modification to change the hydrophobicity of the material. Techniques like plasma treatment or deposition (mainly plasma spraying of Ti and/or thermal plasma coating of hydroxyapatite) as well as wet chemistry[132-136] are commonly used.[137] The most powerful method is coating of the hydrophobic PEEK with a hydrophilic polymer. In that way, an entire new surface layer is added to the substrate. The experimental details for grafting of PEGMA *from* PEEK are shown in *Appendix B*.

7.1 Results and discussion

The surface of PEEK was functionalized by covalently bonding of hydrophilic polymer grafts of PEGMA from initiator-modified PEEK using SI-ATRP. Surface reduction of PEEK to form hydroxyl groups[134] (Figure 7.1) was performed prior to the attachment of 2-bromoisobutyrate initiating groups (Figure 7.2). The reduction of the ketone groups with sodium borohydride in DMSO at 120 ºC did not dissolve the films which makes the method very useful for implantable devices e.g. spinal implants, orthopedic bearing and hip stem material.[137]

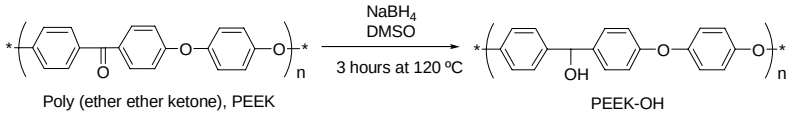

Figure 7.1 Activation of the PEEK surface with sodium borohydride.

SI-ATRP of the monomer PEGMA was performed in aqueous media in the presence of the catalyst system 2,2'-bipyridine and copper chloride. The same ATRP conditions have been used with the initiator, ethyl 2-bromoisobutyrate and without substrates. Moreover, water has been replaced with methanol and the homopolymerizations only resulted in a gel when performed in water but not in methanol. The gel formation strongly indicates that polymer chains have reacted with each other and formed crosslinks. Therefore, the poly(PEGMA) grafts were presumably also crosslinked. Further characterization has only been performed on grafts prepared by SI-ATRP of PEGMA in water.

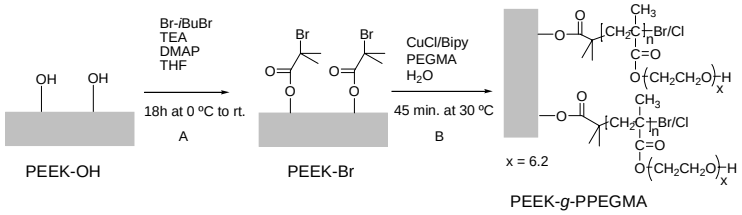

Figure 7.2 (A) Anchoring of the initiating groups on the hydroxyl-functionalized surface; (B) grafting of poly(PEGMA) grafts from the PEEK films using SI-ATRP.

ATR FTIR spectra (Figure 7.3) were compared during the modification of PEEK. The formation of hydroxyl groups was observed as an C-O absorption band appearing at 1057 cm^{-1}. The carbonyl (C=O) absorption band from ester groups at 1736 cm^{-1} indicated the presence of initiating groups on the PEEK surface. This means that it was actually possible to observe absorption bands from the initiating groups on PEEK as opposed to unsuccessful attempts with many other substrates.[44,49,138] For these polymeric substrates ATR FTIR spectroscopy has only been used for characterization of the polymer grafts as an indirect proof for the formation of the initiating groups. Grafting of poly(PEGMA) from the surface resulted in an increase of the C=O band (broad band at 1730 cm^{-1}). ATR FTIR spectroscopy penetrates a few micrometers into the sample; therefore, the spectra of the PEEK-*g*-PPEGMA films contained absorption bands from both poly(PEGMA) and the substrate. Since the ketones in PEEK are conjugated with two aromatic rings the absorption band for C=O appears at 1647 cm^{-1}. Moreover, the C=C ring stretch absorptions from the aromatic rings occur in pairs at 1594 cm^{-1} and 1487 cm^{-1}. The spectra in Figure 7.3 also display C-O-C stretching bands for the aryl ethers in PEEK at 1217, 1185, and 1157 cm^{-1}. All spectra contained the characteristic absorption bands from PEEK which strongly suggests that only the PEEK surface has been modified.

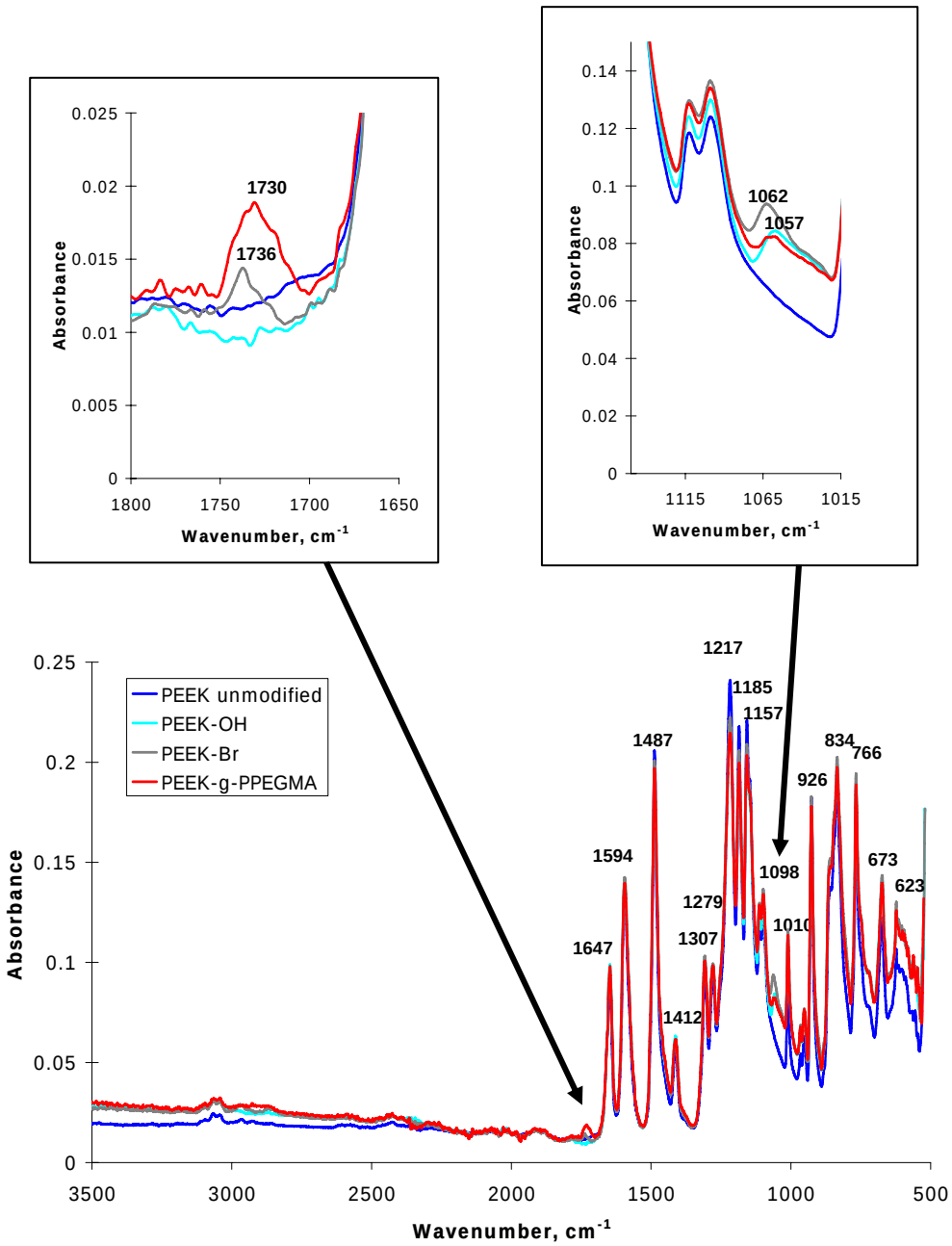

Figure 7.3 FT-IR spectra of the unmodified and modified PEEK films.

The advancing and receding WCAs decreased as the films were modified, reflecting the high hydrophilicity of the hydroxyl groups and poly(PEGMA) (Table 7.1). For the unmodified PEEK and the PEEK with poly(PEGMA) grafts the WCAs of the smooth and the rough side were compared. As expected it was observed that the contact angle hysteresis was larger for the rough side due to the enhanced surface roughness and possibly also surface heterogeneity. The rough side had uniform stripes from the calendaring process which may have caused a heterogeneous

dispersion of the initiating groups and by that means the polymer grafts have been placed with some irregularity. Therefore, the WCAs for the smooth side should be compared in order to evaluate the influence of the modifications. The contact angle hysteresis was unchanged when the ketones on the surface were reduced to hydroxyl groups. However, the formation of initiating sites lowered the hysteresis as the surface became more hydrophobic. The grafting of poly(PEGMA) from the surface increased the hysteresis due to hydrophilic ethylene glycol units in the side chains of poly(PEGMA). Thus, the WCA measurements seem to strongly support the chemical modifications.

Table 7.1 Advancing (adv.) and receding (rec.) water contact angles measured on the smooth (S) or rough (R) side of the unmodified and modified PEEK films.

Material	S/R	WCA (adv.), °	WCA (rec.), °	Δ, °
PEEK	S	99 ± 2	58 ± 4	41 ± 4
PEEK	R	103 ± 3	27 ± 4	76 ± 5
PEEK-OH	S	79 ± 5	38 ± 3	41 ± 6
PEEK-Br	S	92 ±7	59 ± 5	33 ± 9
PEEK-*g*-PPEGMA	S	62 ± 1	25 ± 2	37 ± 2
PEEK-*g*-PPEGMA	R	68 ± 2	19 ± 4	49 ± 4

AFM analysis was additionally employed to evaluate the surface topography of the unmodified and the poly(PEGMA) grafted PEEK surfaces as shown in Figure 7.4. The determined roughness average (R_a) and root mean square roughness (R_q) of the rough side of the films are listed in Table 7.2. The measurements have been made on the rough side of the films as it was more uniform. Scratches on the smooth side of the film from the calendaring process or handling of the film made it impossible to obtain reliable values on that side. The AFM results showed that grafting of poly(PEGMA) from the surface did not change the surface roughness significantly on the rough side. This was an important finding as surface roughness is expected to influence the adsorption of proteins. However, the smooth side will be of most interest for biological applications as it is known that even at the nanometer scale the roughness of the surface has a significant impact on protein adsorption. Thus more proteins will adsorb if the surface roughness is increased.[139] The grafts are expected to be evenly distributed on both sides; therefore, a smooth PEEK surface without any scratches will presumably not be rougher after SI-ATRP of PEGMA.

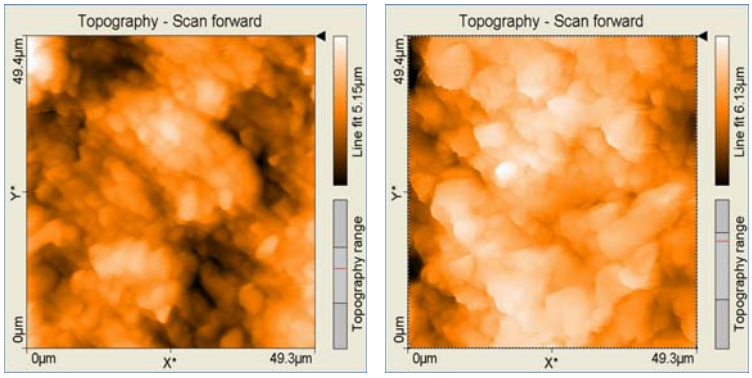

Figure 7.4 AFM images of unmodified PEEK (left) and PEEK-*g*-PPEGMA (right).

Table 7.2 AFM analyses on the rough side of unmodified PEEK and PEEK-*g*-PPEGMA.

Roughness	PEEK	PEEK-*g*-PPEGMA
R_a (µm)	0.76 ± 0.12	0.79 ± 0.18
R_q (µm)	0.94 ± 0.14	1.0 ± 0.2

Thermal analysis made on unmodified PEEK, PEEK-*g*-PPEGMA, and poly(PEGMA) homopolymer confirmed the presence of poly(PEGMA) grafted from PEEK. The thermograms in Figure 7.5 showed that the poly(PEGMA) homopolymer started to decompose around 75 °C and total thermal decomposition was accomplished around 450 ºC. On the other hand, the decomposition of PEEK begins well above 500 °C. Therefore, the 2-3 % weight loss below 500 ºC for the PEEK-*g*-PPEGMA film originated from poly(PEGMA). To our surprise the thermograms for PEEK and PEEK-*g*-poly(PEGMA) cross at about 600 ºC and we do not have a good explanation for this observation.

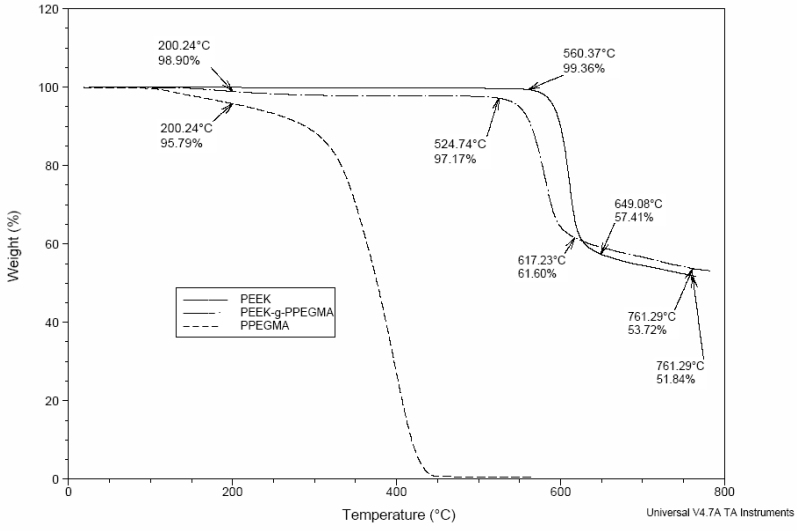

Figure 7.5 TGA of unmodified PEEK, poly(PEGMA) homopolymer (PPEGMA), and PEEK-*g*-PPEGMA.

XPS has been used to investigate the PEEK surface functionalization. Scan survey spectra were used to identify and quantify the elements in the modified PEEK samples. The results are collected in Table 7.3 where also the C/O ratio was calculated in order to follow the modification steps. When poly(PEGMA) was grafted from the surface the C/O ratio was lowered as a consequence of the increased oxygen content in the grafts.

Table 7.3 XPS analyses of the PEEK samples.

Element (%)	PEEK	PEEK-OH	PEEK-Br	PEEK-*g*-PPEGMA	Calc. poly(PEGMA)
C	93.7	84.3	82.9	70.5	64
O	6.3	15.7	15.6	29.5	32
Br			1.6		4
C/O ratio	15.0	5.4	5.3	2.4	2

Chemical composition information was obtained from high resolution scans (Table 7.4). The ketones on the surface of the PEEK films were reduced to hydroxyl groups. Therefore, C=O was not detected for PEEK-OH. This was previously also observed by Noiset *et al.*[134] When the initiating sites were introduced O=C was found due to the ester groups from Br-*i*BuBr. For the poly(PEGMA) grafts the content of C-O increased as the PEG side chains contains ethers. XPS analysis on PEEK-*g*-PPEGMA confirmed that the PEEK surface was modified with poly(PEGMA) as the measured chemical composition only resembles that of the poly(PEGMA) brushes. Taken the penetration of the X-rays in XPS into account this implies that the poly(PEGMA) layer is more than 10 nm.

Table 7.4 Chemical composition information from XPS.

Binding Energy, eV	Attribution	PEEK, %	PEEK-OH, %	PEEK-Br, %	PEEK-*g*-PPEGMA, %
284.3-284.9	C-C (C1s)	90.3	77.4	72.0	42.5
285.3-286.5	C-O (C1s)	8.0	17.0	20.7	50.4
288.3-289.0	C=O (C1s)	*		*	7.0
<283.9 or >287.7	Residual	1.7	5.6	3.0	
530.8-531.9	O=C (O1s)	82.3		50.8	3.5
532.5	O-H (O1s)		*		77.4
532.6-533.5	O-C (O1s)	11.4	97.9	49.2	14.4
<530.4 or >534.1	Residual	6.4	2.1		4.7

* the program was unable to resolve the peaks

The hydrophilic poly(PEGMA) grafts have different applications within the biomedical field as they can be used to avoid non-specific fouling (Figure 7.6). When PEEK-*g*-PPEGMA is pulled out of a protein solution, proteins should not be adsorbed to the surface.

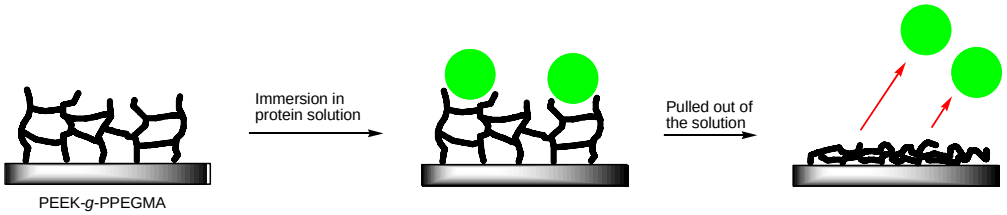

Figure 7.6 The crosslinked poly(PEGMA) grafts on PEEK are expected to repel proteins when the plates are removed from a protein solution.

Confocal fluorescence microscopy has been applied to investigate whether proteins labelled with a fluorophore would adsorb to the poly(PEGMA) surface. Unfortunately, PEEK exhibits autofluorescence at all the employed wavelengths (405, 445, 488, 555, and 639 nm) which makes it impossible to obtain good images of unmodified and modified PEEK exposed to fluorescenced proteins. However, poly(PEGMA) grafted from both polymeric and metallic substrates using SI-ATRP has previously been reported as a non-fouling material.[48,51,105,112-117]

7.2 Conclusions

Polymer brushes of poly(PEGMA) were grafted from PEEK films by use of Surface-Initiated ATRP. The water contact angles were lower for the modified PEEK films; thus hydrophilization of PEEK was achieved. AFM analyses showed that the surface modification did not change the surface roughness. The C/O ratio as well as data from the high resolution XPS confirmed the grafting from the PEEK films. The hydrophilicity of the material, PEEK-*g*-poly(PEGMA) makes it applicable for inhibition of non-specific fouling.

8 Hydrophilization of polypropylene

PP is a substrate of interest for pharmaceutical packaging and delivery systems due to its resistance to most chemicals, high fatigue strength, and good processability. However, PP is hydrophobic like most commercially available thermoplastics, which makes it less compatible with proteins compared to hydrophilic polymers.[12-14] Therefore, the aim was to graft hydrophilic polymer chains from a PP substrate in order to improve the compatibility with an insulin formulation. Plates of PP with the dimensions 3.5 cm x 0.6 cm x 0.1 cm were injection moulded. Modifications of initiator functionalized PP plates were carried out in two rounds. At first PEGMA and DMAAm were applied under conventional SI-ATRP conditions. PEGMA was selected as coatings of poly(ethylene glycol) (PEG) are known to inhibit non-specific fouling due to their water solubility, hydrophilicity, and chain mobility.[12-14,140] Poly(DMAAm) was of interest as it has been grafted from chromatographic packing material and prevented fouling during separation of proteins.[47] Trace of copper was found in the insulin which had been in contact with PP-*g*-PDMAAm. The amides in poly(DMAAm) have probably formed complexes with copper which made it difficult to remove the catalyst. Copper was expected to have an impact on the stability of insulin; therefore, it was decided to minimize the amount of copper catalyst for the polymerizations of M_4PEGMA and M_{23}PEGMA. The MPEGMA monomers were chosen for the same reasons as PEGMA; moreover, methoxy groups were claimed to be more stable then hydroxyl[14] and long-term stability of the coating is essential. ARGET SI-ATRP was selected for the second experimental round which lowered the amount of copper catalyst. Moreover, the method to apply the UV sensitive initiator, benzophenonyl 2-bromoisobutyrate (BP-*i*BuBr) was changed as a visible heterogeneous distribution of the poly(DMAAm) layer was observed. Initially, the PP plates were immersed in the UV initiator which was dissolved in toluene; followed by drying on the edge of a Petri dish. The immersion procedure was performed three times before the plates were irradiated with UV light. The new method involved a spin coating like procedure which will be outlined below. The experimental procedures used for the modifications with the monomers, PEGMA and DMAAm are described in *Appendix C*. The preparation of the samples for the stability studies were carried out according to the description in *Appendix D*. However, a few pictures will be shown below to visualize grafting *from* performed with DMAAm and MPEGMA, respectively. The sample preparation for the stability study is also shown. Table 8.1 summarizes the monomers from the two studies and the catalytical methods which have been applied as well as where the detailed descriptions can be found.

Table 8.1 Overview of modifications and studies made with PP and where to find the detailed descriptions.

Monomer	Catalytical method	Experimental procedure	Adsorption investigations	Stability study
PEGMA	Conventional SI-ATRP	*Appendix C*	x	1st
DMAAm	Conventional SI-ATRP	*Appendix C*	x	1st
M_4PEGMA	ARGET SI-ATRP	8.1.2	x	2nd
M_{23}PEGMA	ARGET SI-ATRP	8.1.3	x	2nd

8.1 Materials and methods

The PP plates were cleaned with ethanol followed by acetone. After drying under vacuum the PP plates were coated with the UV initiator (10 mg/mL in toluene). The residue from the inlet in the mould was mounted in a mechanical stirrer (Figure 8.1). Immediately after immersion in the UV initiator solution the mechanical stirrer was switched on at the maximum rotation (approximately 2000 rounds per minute). The spinning was carried out for 30 seconds. The entire procedure was performed three times per piece which contained four PP plates. The irradiation and removal of unreacted UV initiator were carried out as described previously.

Figure 8.1 "Spin coating" of the UV initiator onto four PP plates.

Polymerizations of MPEGMA n= 4 and 23 from the 188 initiator-modified PP (PP-Br) plates were performed in mixtures of water and methanol.

8.1.1 Chemicals

L-Ascorbic acid (AsA, 99%) 2,2'-bipyridine (Bipy, 99%), copper(II) bromide ($CuBr_2$, 99%), methanol (MeOH, analytical grade), poly(ethylene glycol)methyl ether methacrylate (M_4PEGMA, M_n ~ 300), and poly(ethylene glycol)methyl ether methacrylate (M_{23}PEGMA, M_n ~ 1100) were used as supplied by Sigma-Aldrich. Acetone (99%, Riedel-de-Haën), ethanol (99.9% vol., Kemetyl), and ultra pure water were used without further purification.

8.1.2 ARGET SI-ATRP of M_4PEGMA

(180 mL, 0.63 mol) M_4PEGMA, 120 mL ultra pure water, and 60 mL MeOH were added to a reactor. Nitrogen was bubbled through the mixture for 60

min. 188 PP-Br plates and two PP plates (blank samples) were added and the bubbling with nitrogen was proceeded for 45 min, followed by cooling on an ice bath and bubbling with nitrogen for 15 min. The reactor was kept on ice while $CuBr_2$ (22.7 mg, 0.10 mmol) and Bipy (151.1 mg, 0.96 mmol) were added. The bubbling with nitrogen was continued for 25 min. Finally, the reducing agent, AsA (170.0 mg, 0.96 mmol) was added. The polymerization was carried out at 30 ºC for 30 min. Afterwards the reaction mixture including the PP-*g*-PM_4PEGMA plates were transferred to a 2:1 mixture of water/MeOH. The modified plates were washed in water/MeOH 1:1 for 1 hour and in water/ethanol 5:1 overnight.

8.1.3 ARGET SI-ATRP of M_{23}PEGMA

(198.156 g, 0.18 mol) M_{23}PEGMA was dissolved in 360 mL ultra pure water and 180 mL MeOH. The mixture was bubbled with nitrogen for 45 min. 188 PP-Br plates and two PP plates (blank samples) were added and the nitrogen bubbling was continued for 30 min. The reactor was cooled on ice and bubbled with nitrogen for 15 min. $CuBr_2$ (23.3 mg, 0.10 mmol) and Bipy (158.0 mg, 1.0 mmol) were added while the reactor was kept on ice. Nitrogen was bubbled through for 30 min. Subsequently, the reducing agent, AsA (178.6 mg, 1.0 mmol) was added and polymerization was performed at 30 ºC for 30 min. The reaction mixture including the PP-*g*-PM_{23}PEGMA plates were eventually transferred to about 1.2 L water/MeOH 2:1. Washing of the modified plates consisted of two steps each for one hour 1) 1:1 water/MeOH and 2) 5:1 water/ethanol.

8.1.4 Visualization of the surface modifications

SI-ATRP of DMAAm from 200 initiator modified PP plates is shown in Figure 8.2. Initially, the monomer was distilled under vacuum. Two freeze-pump-thaw cycles were performed for the monomer and three for the other components in order to remove oxygen. The monomer was transferred by cannulation to the flask containing the plates and the catalyst system. Subsequently the polymerization was performed at elevated temperature. At the end of the reaction the catalyst system and the residual monomer were removed by washing of the plates.

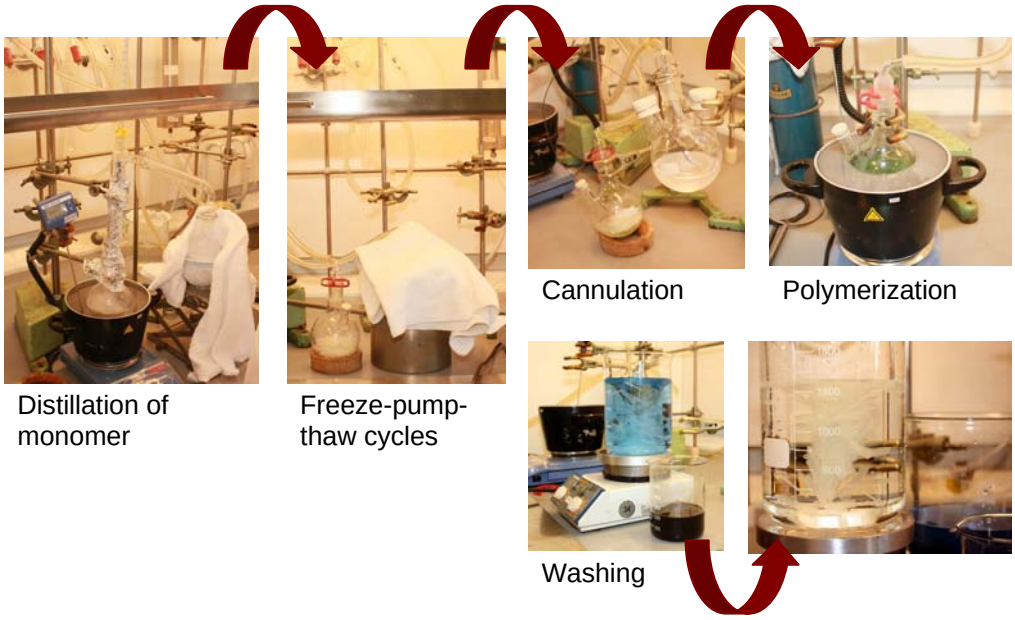

Figure 8.2 Polymerization of DMAAm from 200 PP-Br plates.

The polymerization of PEGMA from 200 initiator functionalized PP plates was performed by Monika Butrimaité in her master project. Removal of oxygen was done by bubbling with nitrogen (pictures not shown). The visual presentation of ARGET SI-ATRP of M_4PEGMA and M_{23}PEGMA was similar; therefore, the procedure in Figure 8.3 represented both monomers. Oxygen in the system was removed by bubbling with nitrogen. When the catalyst, $CuBr_2$ and the ligand, Bipy were added the colour was pale blue. The addition of the reducing agent, AsA changed the colour from blue to brown by reducing Cu^{II} to Cu^{I}. Subsequently, the polymerization was carried out above room temperature. The modified plates were cleaned by several washing steps. The waste from the washing was not colourful as for the conventional SI-ATRP due the change in the catalytic method.

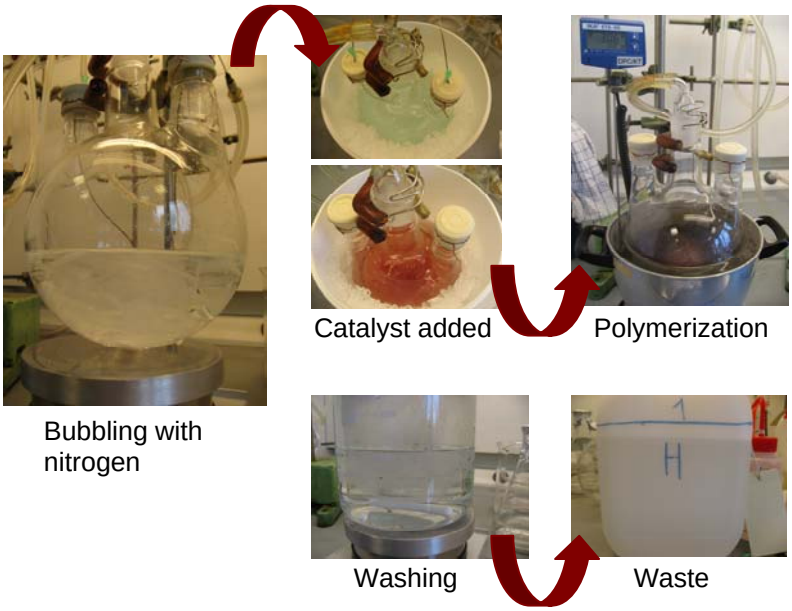

Figure 8.3 The general modification procedure for grafting of the MPEGMA monomers *from* 188 PP-Br plates.

8.1.5 Scanning electron microscope analysis

Images of the plates and insulin fibrils were obtained with conventional SEM and Field Emission SEM (FESEM), respectively. A coating of sputtered platinum was applied to the plates prior to SEM analysis with a Helios NanoLab™ dual beam, focused ion beam FIB-SEM from FEI. The samples were analyzed with a voltage of 5kV and a beam current of 21 pA. Moreover, the samples were tilted 51 degree. A droplet of the insulin fibrils from a 96-well microplate were placed directly on the SEM stub without drying. The images were obtained with beam deceleration on a Nova NanoSEM from FEI. The following settings were applied voltage 6.0 kV, beam current 15 pA, working distance 5-6 mm, beam landing energy 2.0 kV, immersion ratio 3.00, and a low voltage high contrast detector.

8.2 Modification of polypropylene

Initiating groups for ATRP were first anchored on the PP surface before the graft polymerization could take place. Covalent C-C bonds were formed between the initiator and PP when irradiated with UV light at 365 nm. Hydrophilic chains of either poly(PEGMA) or poly(DMAAm) were grafted from the initiator modified PP surface by SI-ATRP (Figure 8.4).

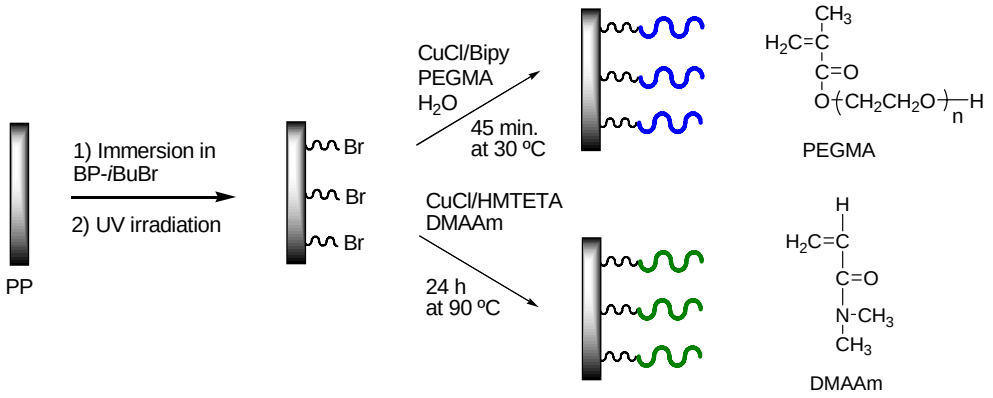

Figure 8.4 Grafting of poly(PEGMA), n = 6.2 and poly(DMAAm) from the initiator functionalized PP surface.

The poly(MPEGMA) grafts n = 4 and 23, respectively were prepared by ARGET SI-ATRP. Moreover, the PP plates were coated with the UV initiator in a slightly more sophisticated way to avoid heterogeneous distribution of the poly(MPEGMA) layer (Figure 8.5). The procedures for the two MPEGMA monomers look identical; however, the ratio between monomer:H_2O:MeOH differed. For M_4PEGMA it was 3:2:1 whereas the mixture with M_{23}PEGMA contained 1:2:1. The content of solvent was increased for M_{23}PEGMA due to poor solubility of the monomer.

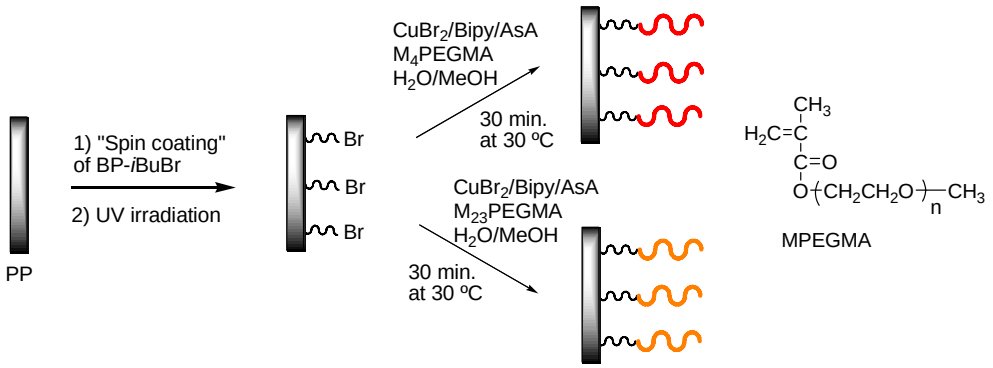

Figure 8.5 Simplified scheme of MPEGMA with 4 and 23 EO units, respectively in the side chain were grafted from PP by ARGET SI-ATRP.

From the ATR FTIR spectra (Figure 8.6) the presence of the poly(PEGMA), poly(DMAAm), and poly(MPEGMA) grafts on the PP substrates were observed. The carbonyl group (C=O) from the ester in the initiator and poly(PEGMA) resulted in a stretching band at 1734 cm^{-1}. Surprisingly, the C=O stretching bands were not visable for the plates with poly(MPEGMA) grafts. The C=O absorption band from the amide in poly(DMAAm) appeared at 1634 cm^{-1}. At 1256 cm^{-1} the C-O and C-N stretching bands were observed which were from the amide in poly(DMAAm) and the O=C-O in initiator, poly(PEGMA) and poly(MPEGMA). The C-O

stretching from O=C-CH_2-CH_2-O-CH_2- (the "alcohol" part) resulted in an increase of the absorption band at 1101 cm^{-1}.

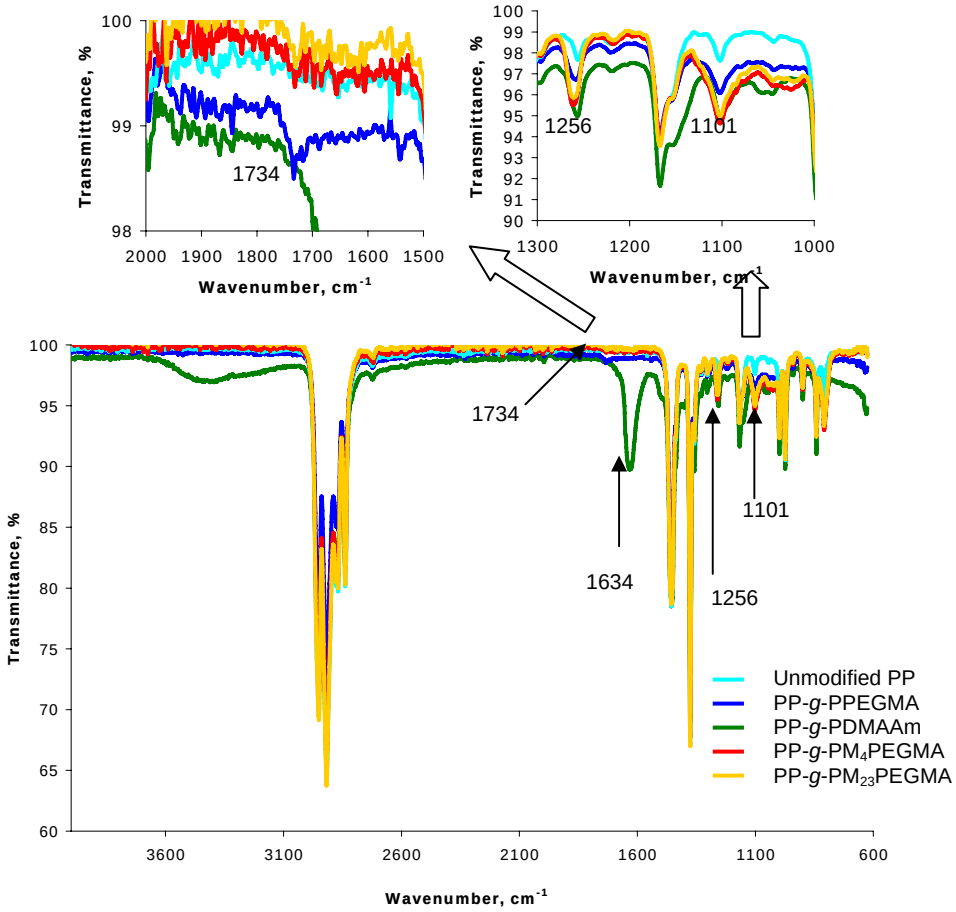

Figure 8.6 ATR FTIR spectra of the modified and unmodified PP.

WCAs were measured on unmodified PP and PP with the hydrophilic grafts of poly(PEGMA), poly(DMAAm) or poly(MPEGMA). The poly(PEGMA), poly(DMAAm), and poly(M_{23}PEGMA) grafts lowered the advancing and receding contact angles significantly. The decrease in WCAs for the PP-*g*-PM_4PEGMA was less pronounced which might be due the shorter side chains and the methoxy end-groups. The results in Table 8.2 show that in all cases the advancing and receding WCAs decreased. The grafting of poly(PEGMA), poly(DMAAm) or poly(M_{23}PEGMA) from the surface also increased the hysteresis due to the hydrophilicity of the grafts. Thus, the WCAs corroborate the significant change in the grafted PP surface properties.

Table 8.2 Dynamic WCA measurements on unmodified and modified PP.

Material	WCA (advancing), º	WCA (receding), º	Δ, °
PP	112 ± 1	87 ± 4	25 ± 4
PP-*g*-PPEGMA	83 ± 3	43 ± 2	40 ± 4
PP-*g*-PDMAAm	104 ± 2	49 ± 3	55 ± 3
PP-*g*-PM_4PEGMA	106 ± 1	84 ± 3	22 ± 3
PP-*g*-PM_{23}PEGMA	91 ± 1	39 ± 1	52 ± 1

8.2.1 Adsorption studies with labelled insulin

When the applied ATRP conditions are used in solution it was revealed that some polymer chains have reacted with each other and formed crosslinks. The corresponding polymer brushes will presumably also crosslink.[141] Nevertheless, all polymer grafts (crosslinked or non-crosslinked) were expected to inhibit protein adsorption when the modified substrates were immersed in a protein drug formulation. The proteins should perceive the hydrophilic polymer grafts as the aqueous media surrounding them. Thus the proteins were not supposed to denaturize or undergo conformational changes. Moreover, the proteins should not be physically adsorbed when the modified substrates were removed from the protein drug formulation.

Insulin aspart was labelled with the dye Alexa Fluor® 488 in borate buffer at pH 9.5 in order to use it for adsorption studies with confocal fluorescence microscopy. The conditions were not the same as in the formulation; however, it was not possible to lower pH to around 7 in the applied procedure. SEM images were obtained in order to decide which side was the most suitable for the confocal microscope analysis (Figure 8.7). The nubbly side was chosen as it had a pattern which was easier to bring into focus. The opposite side, the streaky side was applied for the WCA measurements. Modification of PP was not visible with the conventional SEM analysis which was performed (images not shown).

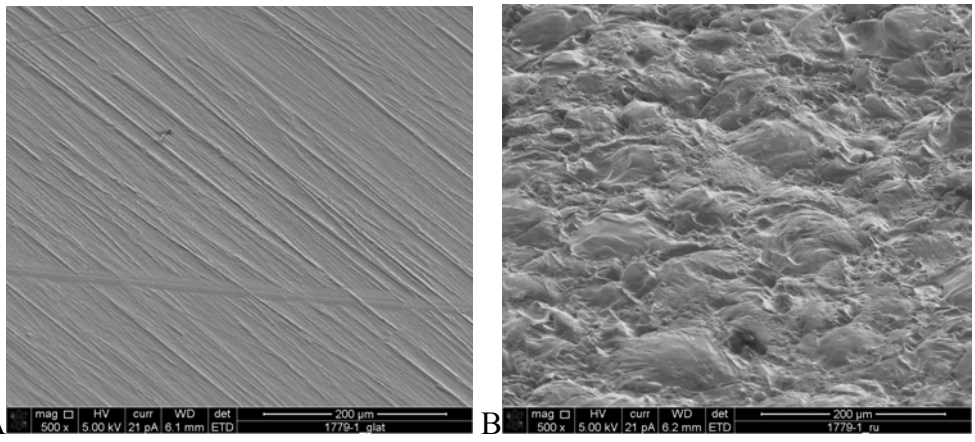

Figure 8.7 SEM images of tilted unmodified PP plates (A) was the streaky side whereas (B) was the nubbly side.

Confocal fluorescence microscopy of modified and unmodified substrates immersed in labelled insulin showed that only PP-*g*-PPEGMA repelled the proteins (Figure 8.8). Samples for confocal fluorescence microscopy were taken out and analyzed after 1, 4, and 24 hours. The areas with adsorbed insulin increased over time on PP-*g*-PDMAAm and PP-*g*-PM_4PEGMA. For the following materials no visible difference was observed between two different exposure times. The images of unmodified PP after 4 hours (B) and 24 hours (C) were similar; moreover, the same observation was made after 1 hour (M) and 4 hours (N) for PP-*g*-PM_{23}PEGMA. The green colour close to edge of the samples (F, J, L, and O) was interpreted as defects in the plates due to the punch out of circular pieces for adsorption studies with labelled insulin. Confocal fluorescence microscopy images were taken to obtain a visual as well as qualitative determination of the adsorbed labelled insulin. A method to measure the amount of adsorbed proteins on the surface has not been developed for the applied confocal microscope.

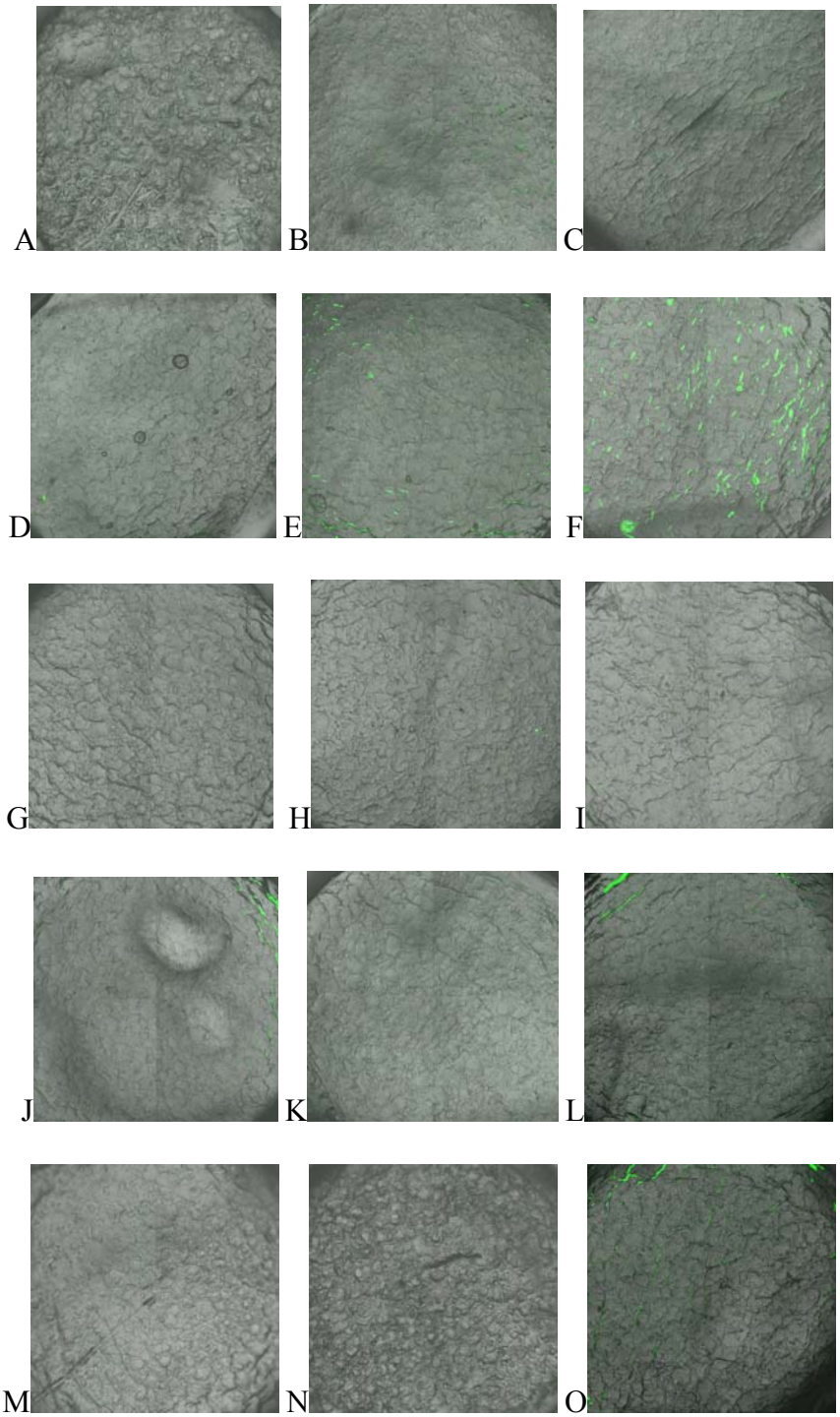

Figure 8.8 Overlay of images from transmission and confocal fluorescence microscopy of substrates immersed in labelled insulin. Unmodified PP after (A) 1 hour, (B) 4 hours, and (C) 24 hours; PP-*g*-PDMAAm after (D) 1 hour, (E) 4 hours, and (F) 24 hours; PP-*g*-PPEGMA after (G) 1 hour, (H) 4 hours, and (I) 24 hours; PP-*g*-PM_4PEGMA after (J) 1 hour, (K) 4 hours, and (L) 24 hours; PP-*g*-PM_{23}PEGMA after (M) 1 hour, (N) 4 hours, and (O) 24 hours.

The efficiency of the crosslinked poly(PEGMA) grafts to repel labelled insulin seemed high and it is expected to be durable for a long time as the grafts are covalently attached to the surface. Adsorption of labelled insulin to unmodified PP, PP-g-PDMAAm, and PP-*g*-PM$_4$PEGMA happened instantly and either the amount of denatured insulin was increased or aggregates were formed. Factors like grafting density of the hydrophilic polymer and the size of the protein will influence the ability to inhibit fouling. Fouling has previously been observed for poly(DMAAm) grafts with low grafting density (in the mushroom regime).[47] The grafting density of poly(DMAAm), poly(PEGMA), and PP-*g*-PM$_4$PEGMA ought to be comparable in this study. It might even be higher for poly(DMAAm) as PEGMA has side chains of about six EO units and M$_4$PEGMA has four. The crosslinked architecture of poly(PEGMA) must make the difference (Figure 8.9).

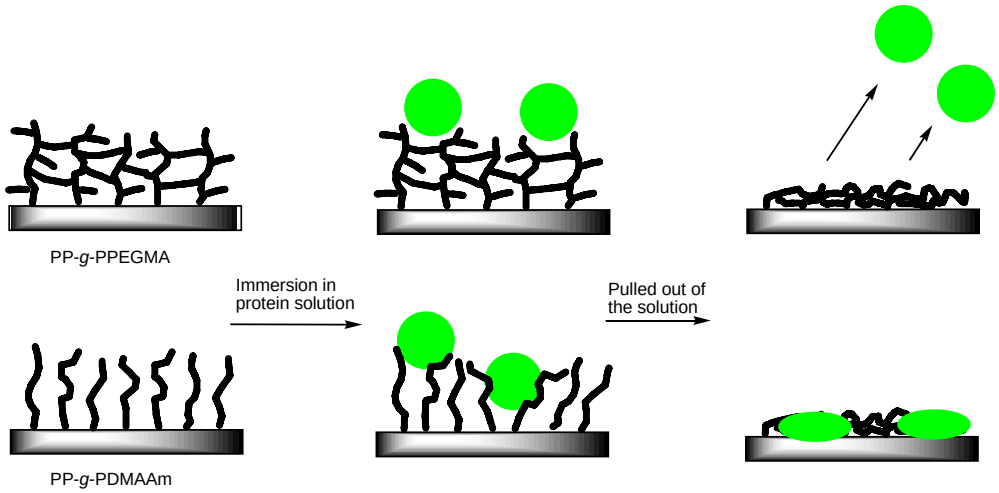

Figure 8.9 Crosslinked hydrophilic grafts of poly(PEGMA) were able to reject labelled insulin whereas insulin adsorbed to the surface with poly(DMAAm) brushes when the substrates were pulled out of a protein solution as visualized.

Rejection of the relatively small size protein, insulin is very dependent on sufficient grafting density or surface coverage in general. Groll *et al.*[15] have compared linear and star PEG coated on silicon substrates with respect to repulsion of insulin and the larger protein, lysozyme. In agreement with theoretical predictions they found that the branched structure of the star PEG and linear PEG with high grafting density could repel insulin. When the grafting density was lower only lysozyme was repelled. Therefore, the crosslinks between the poly(PEGMA) grafts must be able to compensate for a lower grafting density. Moreover, the antifouling properties of poly(DMAAm) could be more dependent of a high grafting density than other protein repellent hydrophilic grafts. The poly(M$_4$PEGMA) grafts showed better repulsion than unmodified PP despite its less hydrophilic character compared with the other modified materials. For M$_{23}$PEGMA the long PEG side chains were expected to give rise to steric hindrance during the polymerization from PP which might result in lower grafting density than for the other polymer

grafts. Adsorption of labelled insulin was only observed for PP-*g*-PM_{23}PEGMA after 24 hours. The long PEG chains could also explain the delay in adsorption of labelled insulin as the transport of insulin to the surface will be influenced by the hydrophilic and water soluble PEG. Nevertheless, adsorption of labelled insulin was observed for both PP-*g*-PM_4PEGMA and PP-*g*-PM_{23}PEGMA (Figure 8.10).

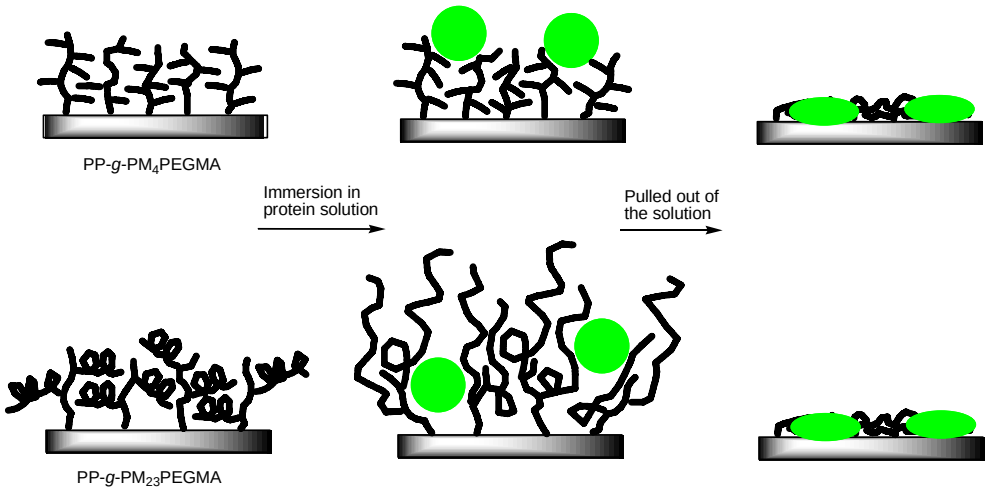

Figure 8.10 Labeled insulin adsorbed to both poly(M_4PEGMA) and poly(M_{23}PEGMA) modified PP; for the PP-*g*-PM_{23}PEGMA the long PEG side chains will presumable delay the adsorption and lower the grafting density.

8.2.2 Conclusions

Poly(PEGMA) and poly(DMAAm) were grafted from PP using SI-ATRP. Grafts of poly(MPEGMA) with n = 4 and 23 were prepared by ARGET SI-ATRP in order to lower the amount of catalyst. Lowering of the WCAs was observed after grafting of the polymer grafts, thus hydrophilization of PP was achieved. ATR FTIR spectra confirmed the modifications of PP with poly(PEGMA), poly(DMAAm), and poly(MPEGMA) grafts. The poly(PEGMA) grafts have presumably crosslinked as previous studies with homopolymerization of PEGMA in water formed a gel. The crosslinked poly(PEGMA) grafts showed excellent repulsion of labelled insulin aspart after 24 hours of exposure. Therefore, the poly(PEGMA) coating has the potential of making polymer materials more usable for devices in contact with protein drug formulations.

8.2.3 Chemical and physical stability of insulin

The compatibility between the hydrophilized PP and insulin was evaluated by comparing the chemical and physical stability of insulin aspart (Asp^{B28} insulin) which has been in contact with the modified and unmodified PP plates. The chemical and physical stability of Asp^{B28} insulin was assessed by two chromatographic methods and Thioflavin T (ThT) test, respectively. The samples for the stability assessments were prepared in Penfill® (Figure 8.11).

Two plates were inserted in each glass cartridge except for blank samples which did not contain any plates. The glass cartridges were equipped with rubber plungers and Asp^{B28} insulin was transferred with a syringe. Finally, the cartridges were closed with caps.

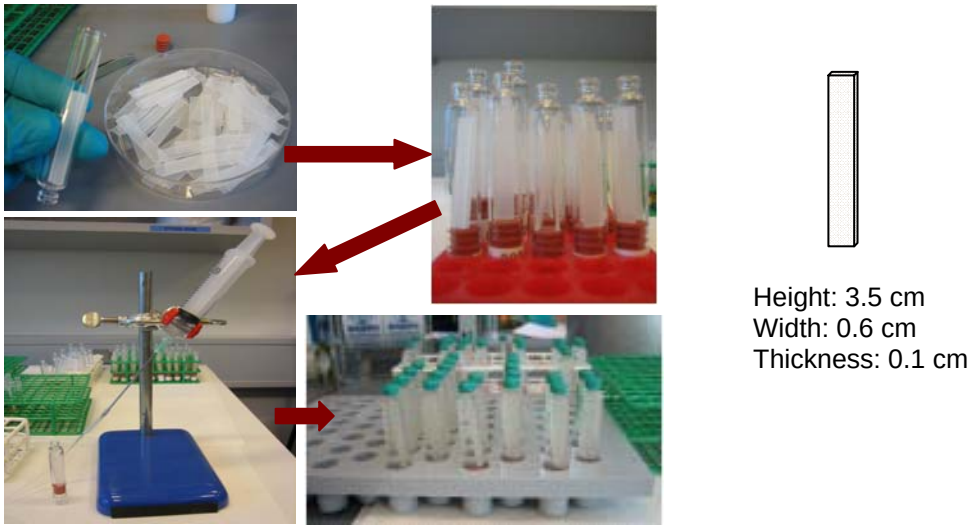

Figure 8.11 Preparation of samples for a stability study.

Asp^{B28} insulin stored in glass (blue cap bottle) was used as a reference because similar results are well-documented. Two studies have been conducted and in both studies the samples have been stored at 5, 20, and 37 °C; however, for the time being the maximum storage time for the samples taken out was 8 months for the first study and 4 months for the second. In the first study PP was coated with the hydrophilic polymer, poly(PEGMA) and poly(DMAAm). The second study included two different types of poly(MPEGMA) grafts with 4 and 23 EO in each monomer unit, respectively. The results from the studies will compare the influence of modified PP with the unmodified PP on the stability of Asp^{B28} insulin. In Table 8.3 the different type of samples are listed.

Table 8.3 List of sample names

Type of samples	Abbreviation	Stored at 5 °C	Stored at 20 °C	Stored at 37 °C
Reference Asp^{B28} insulin	Ref.	Ref.		
Unmodified PP	U	U5	U20	U37
Poly(DMAAm) coating	D	D5	D20	D37
Poly(PEGMA) coating	P	P5	P20	P37
Blank sample	B	B5	B20	B37
Poly(M_4PEGMA) coating	4M	4M5	4M20	4M37
Poly(M_{23}PEGMA) coating	23M	23M5	23M20	23M37

Chemical stability is related to degradation of insulin by covalent changes. The chemical deterioration will result in formation of molecules which may be less active and undesirable. Two types of chemical reactions, intermolecular reactions and hydrolysis are involved in the chemical deterioration. The physical stability of Asp^{B28} insulin was evaluated by the

tendency to form fibrils. When insulin is exposed to e.g. hydrophobic surfaces, heat or shear forces, it can undergo conformational changes which will result in aggregation and formation of insulin fibrils.[142]

SEC and Reverse Phase HPLC (RP-HPLC) methods were applied to determine the amount of Higher Molecular Weight Proteins (HMWP) and the formation of hydrolysis products, respectively. HMWP are degradation products which are hydrophobic and consist of covalent bound dimers and polymers which are formed during storage of the insulin formulation. The covalent bonds were formed by disulfide exchange reactions or aminolysis between two A-chains in the insulin molecules or between an A-chain and a B-chain.[142] The chromatograms from the RP-HPLC analysis also showed the preservative concentrations and assay of insulin in the samples. Each data point on the curves from the HPLC analyses was an average of two samples. However, the standard deviation was not included as the numbers from the two samples showed great resemblance as expected. In the following figures the line combining the measured values should serve as a guide to the eye and does not necessarily reflect values between the reported values. In RP-HPLC the insulin dimers and some oxidation products[143,144] were designated as Asp^{B28} insulin related impurities (Figure 8.12). PP with the poly(DMAAm) coating resulted in the highest content of Asp^{B28} insulin related impurities.

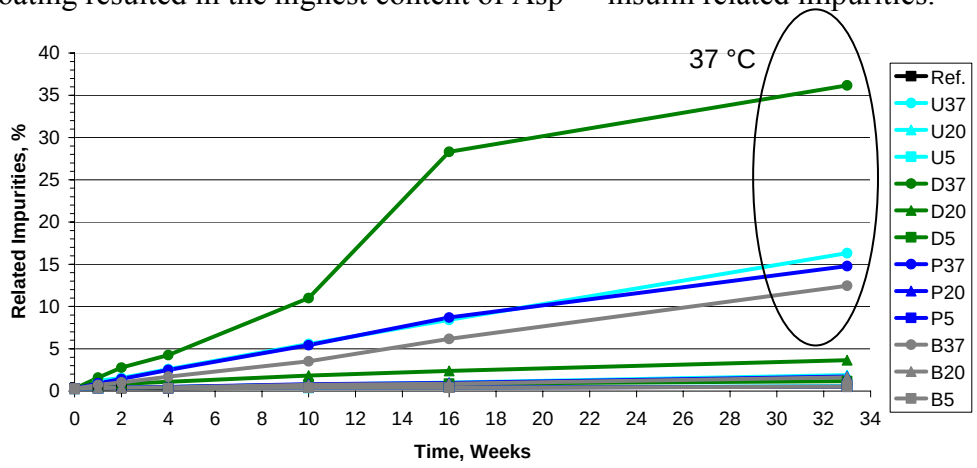

Figure 8.12 Asp^{B28} insulin related impurities in pct. relative to the total area for samples stored at 5, 20, and 37 °C; U=unmodified, D=poly(DMAAm) coating, P=poly(PEGMA) coating, B=blank, and Ref.=reference.

In the second stability study the differences between Asp^{B28} insulin in contact with unmodified PP and poly(MPEGMA) coated PP were less pronounced. After a longer storage like the 8 months for the first study it might be possible to observe larger differences. The content of Asp^{B28} insulin related impurities was slightly higher in the samples with poly(MPEGMA) coated plates stored at 37 °C (Figure 8.13). The change was not large enough to conclude that the poly(MPEGMA) coatings increased the chemical deterioration compared with unmodified PP. In general, the content of Asp^{B28} insulin related impurities in samples was lower in the second stability study compared with the first.

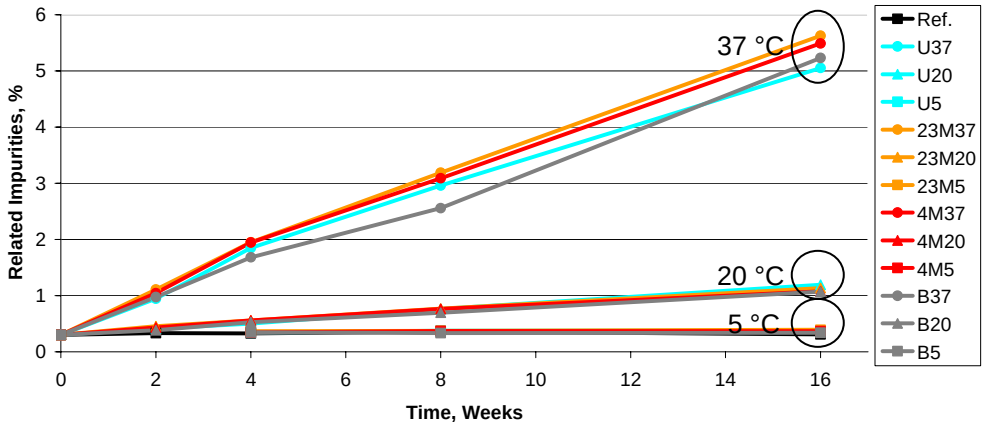

Figure 8.13 Asp^{B28} insulin related impurities from the second stability study in pct. to the total area for samples stored 5, 20, and 37 °C; U=unmodified, 23M=poly(M_{23}PEGMA) coating, 4M=poly(M_4PEGMA) coating, B=blank, and Ref.=reference.

The phenol concentration and pH were not influenced by poly(MPEGMA) coatings. On the hand, major changes were observed due to the poly(DMAAm) coating in the first study. Therefore, results from the first study and possible explanations will be outlined below.

A decrease in the content of phenol is observed in the samples exposed to poly(DMAAm) coating (Figure 8.14). This can either be explained by depletion through adsorption to the poly(DMAAm) coating or by degradation of phenol due to the coating. In any case, it can be concluded that the poly(DMAAm) coating has a high affinity to preservatives in the drug formulation. Asp^{B28} insulin will despite its monomeric character form hexamers in the presence of zinc ions and phenol or phenol-like molecules.[145] The monomers in the hexamer are either in the T or R state. In the T state the residues B1-B9 adopt an elongated conformation whereas they form α-helix in the R state, resulting in one α-helix from B1-B20. Three conformational states are known for the hexamer T_6 (all monomers in the T state), T_3R_3 (monomers alternating between T and R state), and R_6 (all monomers in the R state).[145,146] Insulin binds phenol and the compact and stable R_6 hexamer is formed. If less phenol is present the less stable T_6 will be formed. With the experimental conditions reported by Derewenda *et al.*[146] it was concluded that the phenol concentration had an influence on the physical stability. However, the phenol concentration required for stabilizing the R_6 hexamer[146] is lower than the phenol concentration in the present formulation as phenol here also serves as a preservative. Nevertheless, it can not be ruled out that the shift in the phenol concentration observed in samples exposed to the poly(DMAAm) coating may have an effect on the physical stability of Asp^{B28} insulin.

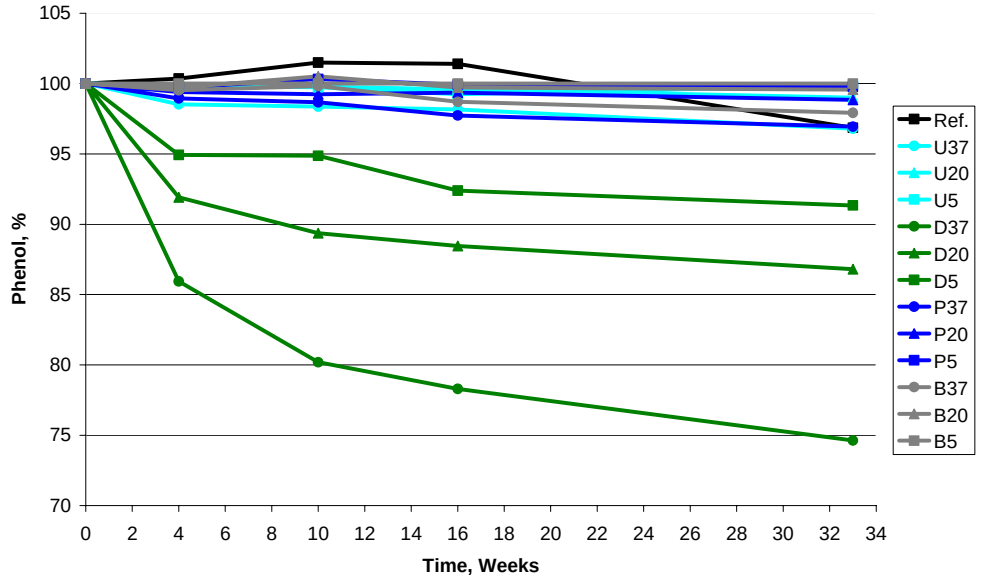

Figure 8.14 Phenol concentration in pct. relative to blank sample for the samples stored at 5, 20, and 37 °C; U=unmodified, D=poly(DMAAm) coating, P=poly(PEGMA) coating, B=blank, and Ref.=reference.

Insulin degrades relatively fast below pH 5 and above pH 8. The optimum pH range for insulin was 6-7. At acidic pH values deamidation at residue A21 and formation of covalent insulin dimers will dominate whereas alkaline pH values will result in disulfide reactions. Formation of covalent insulin dimers and oligomers has an optimum around pH 4 and above pH 9 an accelerated formation of covalent oligomers and polymers was observed due to disulfide interchange reactions. Hydrolysis of insulin has a minimum at pH 6.5.[142] The increase in pH for Asp^{B28} insulin which has been in contact with the poly(DMAAm) coating (Figure 8.15) is consistent with increase in Asp^{B28} insulin related impurities. The content of Asp^{B28} insulin deamidation products (Asp^{B3} + Asp^{A21} + $isoAsp^{B3}$, data not shown) was also higher when it was exposed to poly(DMAAm). The observation confirmed that hydrolysis of insulin will increase if pH is increased from 7.35 to above 8. The increase in the pH value which was observed in the poly(DMAAm) samples might also contribute to stabilization of Asp^{B28} insulin. Changes in pH can be due to leachables. Analysis with Inductive Coupled Plasma Optical Emission Spectroscopy (ICP-OES) showed that Asp^{B28} insulin exposed to the poly(DMAAm) coating and stored at 37 °C for 20 weeks contained 7.2 µM copper (0.46 µg/mL) whereas the potential copper content in other samples was below the detection limit of 0.8 µM (0.05 µg/mL). The copper contamination most likely originates from the catalyst, which is applied for the SI-ATRP. Divalent metal ions are known to be capable of oxidizing insulin and increase pH. A spread of ± 0.3 in the pH values was measured for

some samples containing the poly(DMAAAm) coating and stored at 37 °C which can be due to heterogeneous distribution of the coating.

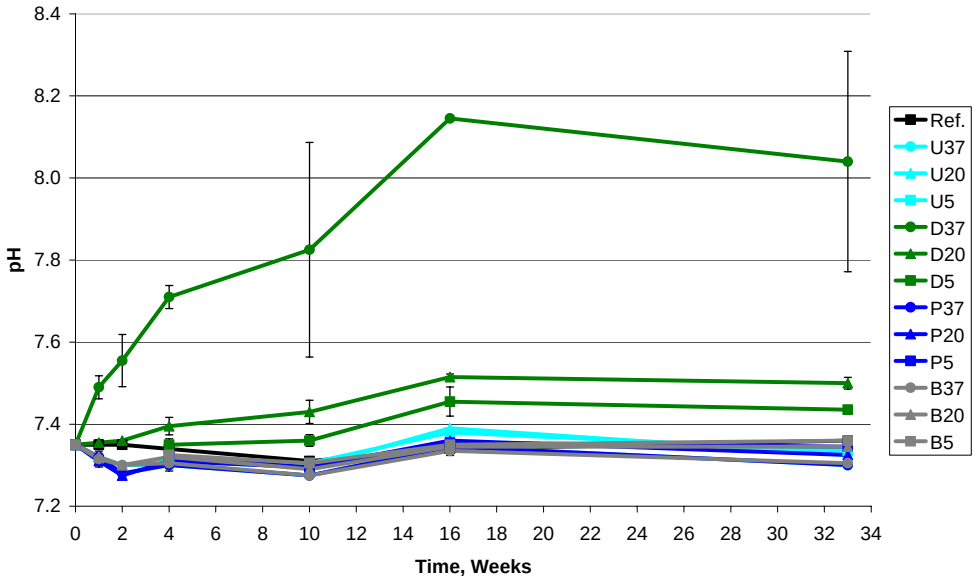

Figure 8.15 pH for all samples stored at 5, 20, and 37 °C; U=unmodified, D=poly(DMAAm) coating, P=poly(PEGMA) coating, B=blank, and Ref.=reference.

To investigate the tendency of insulin to fibrillate the ThT test was used. Insulin which has been exposed to modified or unmodified PP was compared with reference insulin and blank samples. Insulin and the dye ThT was transferred to 96-well microplates and placed in fluorescence plate-reader. ThT will bind to the insulin fibrils and its excitation and emission spectra will be shifted from maxima at 430 and 342 nm to 482 and 442 nm. When insulin fibrillates the ThT fluorescence intensity versus time will form a sigmoidal curve (Figure 8.16) consisting of a lag phase, a growth phase, and an equilibrium phase. From the ThT curve lag time, rate constant, and maximum intensity (I_{max}) can be determined by manual readings. The rate constant was obtained from the slope of the growth phase (Δ(fluorescence intensity)/ΔTime).

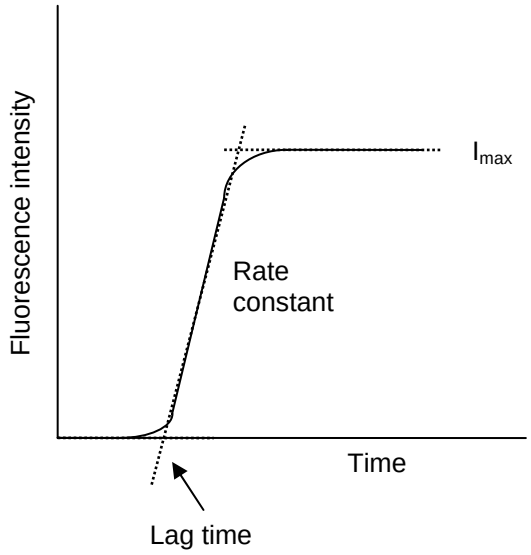

Figure 8.16 Illustration of the increase in fluorescence intensity for ThT when insulin fibrils are formed.

Asp^{B28} insulin exposed to the poly(DMAAm) coating for 16 (shown on Figure 8.17) and 33 weeks at 37 °C (D37) did not reach a I_{max} value and it was impossible to determine the rate constant within the 14 days of testing on the plate-reader. The pH values were above 7.3 for those samples; therefore, the ThT dye might undergo hydroxylation during the time of the measurements.[147] More dye was added to the wells containing D37 which have been stored for 33 weeks. The fluorescence intensity for the D37 samples after 33 weeks was around 1000 a.u. (the initial value for the other 37 °C samples was about 300 and 100 a.u. for the rest) when the test was initiated and it did not increase significantly for an extended period of 21 days. 4 µL of ThT were added to each well three times during this time period; however, only minor increases in the fluorescence intensity were observed. Therefore, the results from the D37 samples have been omitted in Figure 8.18 and Figure 8.19. Some reasons have already been described for the observed increase in physical stability due to the poly(DMAAm) coating and they might interact. Copper from the catalyst has already been mentioned and it is also expected to have a beneficial effect on the physical stability. Studies with amyloid-β (Aβ) peptides have shown that Cu^{II} inhibits $A\beta_{42}$ fibrillation and initiate formation of non-fibrillar $A\beta_{42}$ aggregates. After incubation for a week amyloid fibrils were detected in samples with $A\beta_{42}$ aggregates.[148] If the fibrillation process is slow other studies have shown that metal ions can accelerate the fibril formation by assembly between peptides and metal-induced aggregates.[149] The growth of fibrils is fast for Asp^{B28} insulin; therefore, the copper ions were expected to inhibit fibrillation by lowering the concentration of free insulin, which was not aggregated insulin. The time for ThT test for the samples

stored for 16 weeks was also extended until 21 days and the Asp^{B28} insulin exposed to poly(DMAAm) coating reached a very low I_{max} value compared with other samples. Moreover, the I_{max} values for the Asp^{B28} insulin in contact with unmodified PP or the poly(PEGMA) coating were lower than the blank sample. Differences in the fibril structures could be an explanation; therefore, SEM images of the Asp^{B28} insulin fibrils from the ThT test were compared (Figure 8.17). Asp^{B28} insulin fibrils were observed as thread-like structures which were more compact for (A) – (C) than (D). The difference in the fibrillar structure could explain the lower I_{max} values due to unmodified PP and the poly(PEGMA) coating. Furthermore, (B) contained almost no fibrils. Yoshiike *et al.*[150] reported that Zn^{II} or Cu^{II} prevent β-aggregation i.e. ThT reactive fibril formation. The Cu^{II} present in the poly(DMAAm) sample might therefore not only inhibit the Asp^{B28} insulin fibril formation but also suppress it. If image (B) was compared with the others it looked like the final level of ThT reactive fibrils was suppressed. The suppression of ThT reactive fibrils conformed to the very low I_{max} value for the poly(DMAAm) samples.

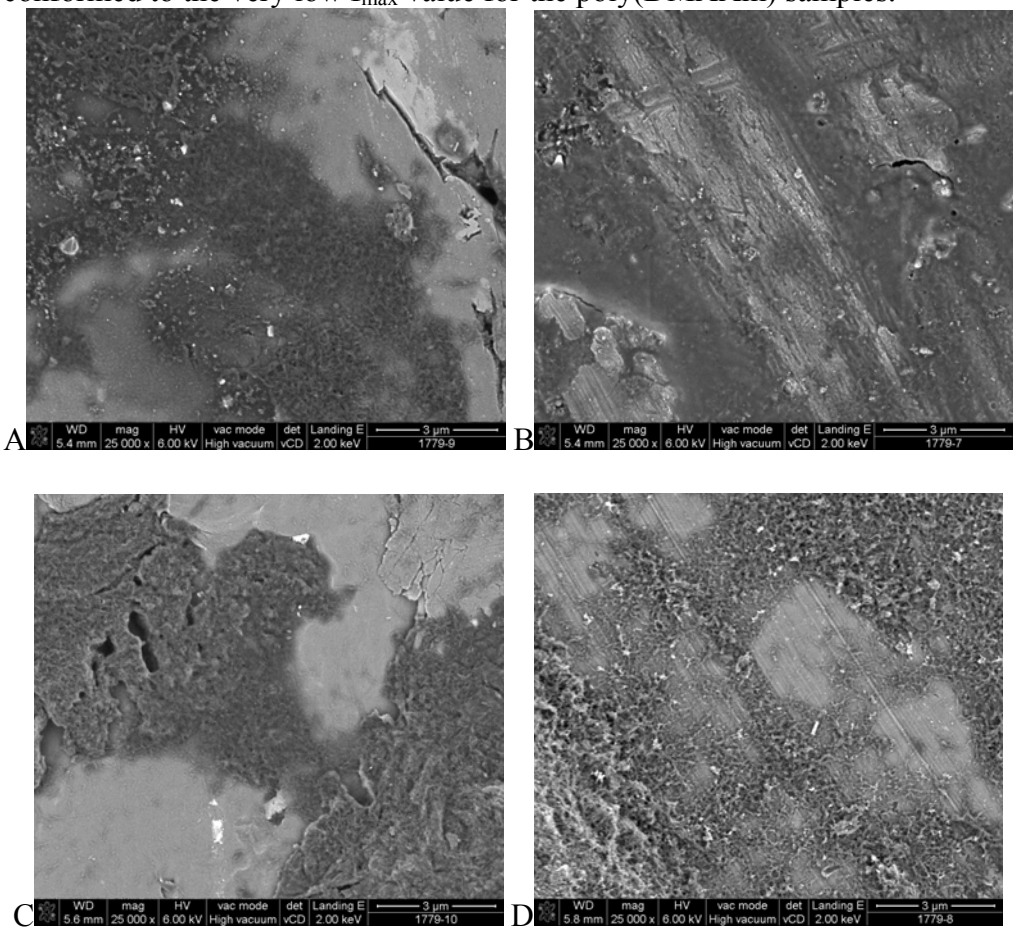

Figure 8.17 SEM images of the Asp^{B28} insulin fibrils from the ThT test; Asp^{B28} insulin has prior to the test been exposed to the unmodified PP (A), the poly(DMAAm) coating (B), the poly(PEGMA) coating (C) and Asp^{B28} insulin from the blank sample (D); all samples have been stored 16 weeks at 37 °C.

Correlations between the rate constant in the ThT assay test and Asp^{B28} insulin related impurities and HMWP were illustrated in Figure 8.18 and Figure 8.19, respectively. The three data points for each type of sample represent the three different times (10, 16, and 33 weeks) where samples were taken for the ThT assay test. The rate constant decreases whereas the content of Asp^{B28} insulin related impurities and HMWP increase over time. If the rate constant was replaced with I_{max} similar correlations were observed. The results for the samples stored at 5 °C have been omitted to elucidate the coherence between chemical and physical stability; however, they were located between the reference and the 20 °C samples.

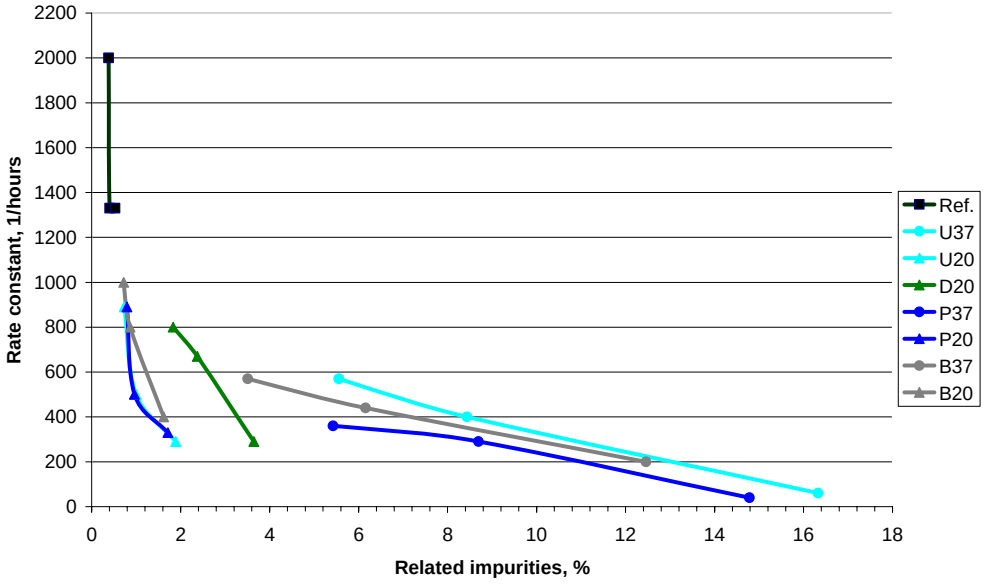

Figure 8.18 The rate constant from the ThT test versus Asp^{B28} insulin related impurities in pct. relative to the total area for the three sampling times 10, 16, and 33 weeks; U=unmodified, D=poly(DMAAm) coating, P=poly(PEGMA) coating, B=blank, and Ref.=reference.

When the rate constant decreased the physical stability was improved as the fibril formation was slowed down (Figure 8.18 and Figure 8.19). Inverse correlations between the content of Asp^{B28} insulin related impurities or HMWP and the tendency to fibrillate were observed. Increased physical stability of Asp^{B28} insulin due to formation of insulin dimers, oligomers, and polymers has previously been reported by Senstius *et al.*[11] The observations with the lower rate constants for a higher content of Asp^{B28} insulin related impurities and HMWP fit in well with the theory about the correlation between chemical and physical stability. Samples with the poly(DMAAm) contained less insulin polymer but more dimer than the other samples kept at the same temperature. Related impurities contain the different covalent bound insulin dimers; therefore, the data for Asp^{B28} insulin exposed to poly(DMAAm) at 20 °C (D20) was separated from the other 20 °C samples in

Figure 8.18. In Figure 8.19 insulin dimers and polymers were added up in HMWP. Thus D20 did not differ from the other 20 °C samples. Moreover, the 37 °C samples seem to indicate a slight improvement in the physical stability due to the poly(PEGMA) coating without jeopardizing the chemical stability as related impurities and HMWP were not higher than for the unmodified PP.

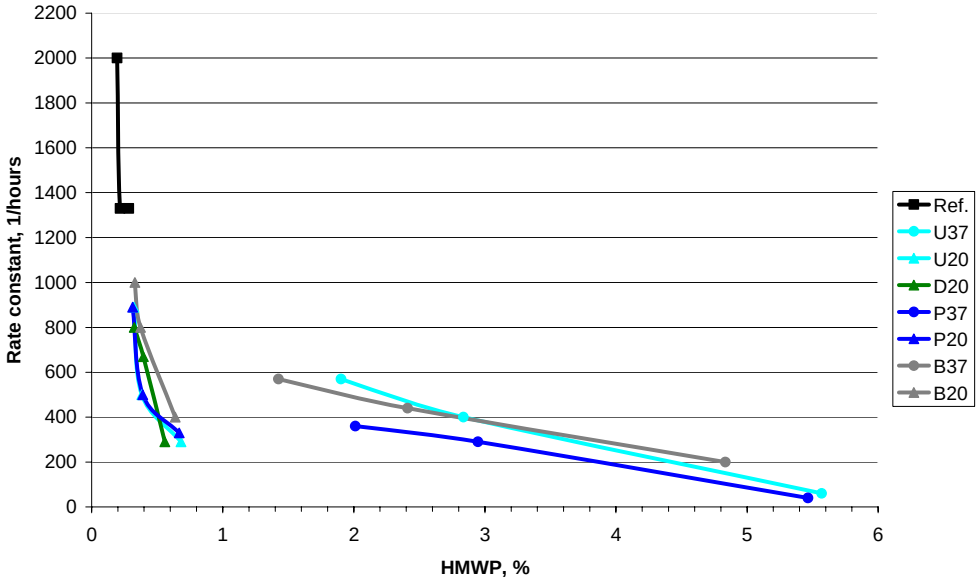

Figure 8.19 The rate constant from the ThT test versus HMWP in pct. relative to the total area for the three sampling times 10, 16, and 33 weeks; U=unmodified, D=poly(DMAAm) coating, P=poly(PEGMA) coating, B=blank, and Ref.=reference.

The same trend between the rate constant and the content of Asp^{B28} insulin related impurities or HMWP seemed to be present for the second stability study. The ThT test was only performed twice after 4 and 16 weeks. The ThT curves, the Asp^{B28} insulin related impurities, and the HMWP for the samples did not vary much after 4 weeks. For that reason more overlap was observed for the first data points compared with second study in which the ThT test was carried out after 10, 16, and 33 weeks. When poly(M_4PEGMA) coated PP was compared with unmodified PP different observations were made for the two storage temperatures, 20 and 37 °C (Figure 8.20). According to the 20 °C samples the poly(M_4PEGMA) coating showed improved physical stability as the fibrillation rate constant after storage for 16 weeks was lower than for unmodified PP. The 37 °C samples did not reveal the same positive effect on the physical stability due to coating. The poly(M_4PEGMA) coating might be applicable if the tendency observed at the lower temperature continues. The poly(M_{23}PEGMA) coating was not more favourable than the unmodified PP with respect to the stability of Asp^{B28} insulin. In short, the poly(M_{23}PEGMA) coating neither improved the Asp^{B28} insulin stability nor deteriorated it more than unmodified PP for the tested time period.

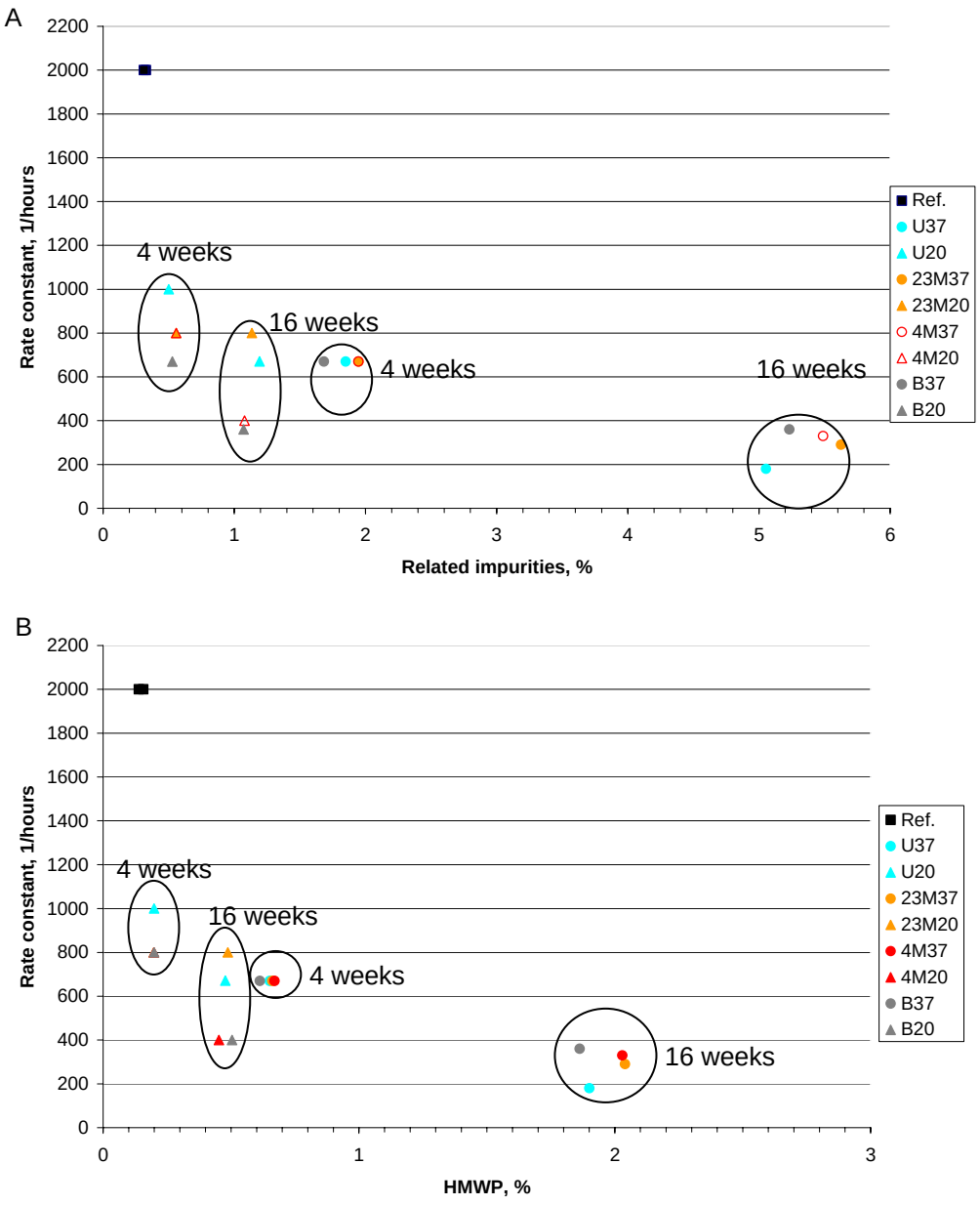

Figure 8.20 The rate constant from the ThT test versus (A) Asp^{B28} insulin related impurities and (B) HMWP in pct. relative to the total area for the two sampling times 4 and 16 weeks; U=unmodified, 23M=poly(M_{23}PEGMA) coating, 4M=poly(M_4PEGMA) coating, B=blank, and Ref.=reference.

8.2.4 Conclusions

In general, Asp^{B28} insulin related impurities and HMWP were observed to correlate inversely with the increased physical stability. Cause and effect have not been clarified; however, the observations pointed towards coherence between the chemical and physical stability of Asp^{B28} insulin. The poly(DMAAm) coating showed a high affinity to the preservatives in

consequence a lower phenol concentration was observed which cannot be excluded to have an effect on the physical stability. Moreover, the poly(DMAAm) resulted in the highest content of Asp^{B28} insulin related impurities. The increase in pH was consistent with the increase in Asp^{B28} insulin related impurities due to poly(DMAAm). 7.2 µM copper from the catalyst was detected in the samples with poly(DMAAm) coated PP and the copper might oxidize insulin and increase pH. It cannot be ruled out that the copper from the catalyst will also contribute to improved physical stability as Cu^{II} is expected to inhibit fibrillation for Asp^{B28} insulin. Finally, the poly(DMAAm) samples contained less Asp^{B28} insulin polymer but more dimer than the other samples kept at the same temperature.

The poly(PEGMA) coating resulted in improved stability of Asp^{B28} insulin compared to unmodified PP and the poly(DMAAm) coating. The improvement of the stability was especially evident for the samples stored at 37 °C when the samples have been stored for eight months. The data observed for the accelerated conditions (37 °C) have the same trend as data observed at 5 and 20 °C. The observed improvement may therefore be expected to be predictive of long term stability at 5 and 20 °C. Poly(PEGMA) coating of PP surfaces in primary packaging materials for Asp^{B28} insulin is thus expected to have a pronounced positive effect on the Asp^{B28} insulin stability.

The influence on the Asp^{B28} insulin stability due to poly(MPEGMA) coatings was vague when it was compared with unmodified PP. Prolonged storage time might give more lucid results. Dependence on the storage temperature was observed when the tendency to form fibrils was compared for poly(M_4PEGMA) coated PP and the unmodified PP. For the 20 °C samples the poly(M_4PEGMA) coating resulted in the lowest fibrillation rate constant whereas the fibrillation rate constant was lower for unmodified PP when the samples were stored at 37 °C. Table 8.4 summarizes the influence of the coatings on the results compared to the unmodified PP.

Table 8.4 Results for Asp^{B28} insulin after exposure to the coated PP compared with unmodified PP; green is a favorable result whereas red is unfavorable; the arrows indicate whether the value increases (↑), decreases (↓) or stays at the same level (→) compared to samples exposed to unmodified PP.

Coating	Asp^{B28} insulin related impurities	HMWP	Fibrillation rate constant	Phenol	pH	Copper
Poly(DMAAm)	↑	↑	↓	↓	↑	↑
Poly(PEGMA)	↓	↓	↓	→	→	→
Poly(M_4PEGMA)	→	→	↓↑	→	→	*
Poly(M_{23}PEGMA)	→	→	↑	→	→	*

* ICP-OES was not performed on the samples in the second stability study.

SEM images of Asp^{B28} insulin fibrils from the first stability study visualized the suppression of fibrillation and changes in the fibrillar structure which in both causes have been observed as lower I_{max} values in the ThT test.

Considerations like sterilization and permeability will have to be considered before PP coated with poly(PEGMA) can be applied in a stability

study which compares the polymeric material with glass. However, this study has proven that a material like poly(PEGMA) coated PP has the possibility of replacing glass for storage of a drug product formulation.

9 Concluding remarks

Hydrophilization of the model substrate, PEEK was achieved by SI-ATRP of PEGMA. The PEEK film acted as a very good model system in the different modifications steps. It was possible to use various characterization methods to confirm the modifications e.g. AFM, TGA, WCA and XPS. ATR-FTIR spectroscopy of initiator functionalized PEEK films even revealed the carbonyl group in the ATRP initiator which was very unique. PEEK-*g*-poly(PEGMA) is applicable for inhibition of non-specific fouling due the hydrophilicity of the material. However, autofluorescence of the material made it impossible to apply confocal fluorescence microscopy to study the expected non-fouling properties.

A benzophenone containing UV initiator was synthesized and applied to prepare PP plates for SI-ATRP. The experimental work with PP plates was carried out in two rounds. Firstly, poly(PEGMA) and poly(DMAAm) were grafted *from* PP by conventional SI-ATRP. Secondly, grafts of poly(MPEGMA) with n = 4 and 23 EO units in the side chains, respectively were prepared by ARGET SI-ATRP in order to decrease the amount of catalyst. It was decided to change the catalytical method as metal analysis by ICP-OES showed that the insulin exposed to PP-*g*-PDMAAm plates contained copper. The presence of the polymer grafts was confirmed with ATR-FTIR spectroscopy. Results from WCA measurements showed that hydrophilization of PP was obtained by preparation of the polymer grafts.

The ability of modified and unmodified PP to repel labelled Asp^{B28} insulin was investigated by confocal fluorescence microscopy. The crosslinked poly(PEGMA) grafts were the only ones which showed excellent repulsion of labelled Asp^{B28} insulin after 24 hours of exposure. Two stability studies were conducted in which the stability of Asp^{B28} insulin in contact with either modified PP or unmodified PP was compared. PP-*g*-PPEGMA and PP-*g*-PDMAAm plates were employed in the first stability study and results after 8 months of storages have been obtained. The second stability study with PP-*g*-PM_4PEGMA and PP-*g*-PM_{23}PEGMA plates was set up after the first and it has been going for 4 months until now. PP with the poly(PEGMA) coating was the only material which resulted in better stability of Asp^{B28} insulin than unmodified PP. The results from the poly(DMAAm) coating showed improved physical stability; however, the chemical stability of Asp^{B28} insulin was very poor. In the tested period the poly(MPEGMA) coatings have not shown significant differences in neither chemical stability nor physical stability compared with unmodified PP.

The overall objective of the PhD project was accomplished as PP-*g*-PPEGMA showed eminent repulsion of labelled Asp^{B28} insulin. Moreover, chemical and physical stability of Asp^{B28} insulin was significantly improved after 8 months of exposure to PP-*g*-PPEGMA compared with unmodified PP.

10 Outlook

Low grafting density could be one of the explanations for the absence of protein repulsion for the poly(DMAAm) and poly(M_4PEGMA). It is possible that the applied UV initiator does not supply enough initiating sites to obtain a sufficient grafting density. Therefore, it would be interesting to try to find a more effective method to activate PP and compare the anti-fouling properties after SI-ATRP.

The poly(PEGMA) grafts can be prepared in methanol without croslinking, thus PEGMA grafting *from* PP should be performed in methanol. An adsorption study with labelled Asp^{B28} insulin is expected to show adsorption on the poly(PEGMA) coating prepared in methanol. If this study is carried out the theory about the anti-fouling crosslinks could be confirmed.

The molecular weight of the polymer grafts has not been determined as it requires a large surface area to have enough material for SEC analysis. It is very time-consuming to modify a large amount of plates with the UV initiator. However, a study in which the molecular weight can be determined has to be carried out either on many of the already applied plates or some larger plates have to be moulded.

Metal analysis of the samples in the second stability studyy is not expected to reveal any copper from the catalyst as the stability of Asp^{B28} insulin has not changed significantly during the first four months. However, in order to confirm that copper from the catalyst is not present ICP-OES should be performed.

Further investigations of the poly(PEGMA) coated PP have to be made before the material can be used for container or devices in contact with insulin. Sterilization of PP-*g*-PPEGMA by e.g. steam should be performed and any impact on e.g. the shape, transparency, and the mechanical properties should not be observed. Moreover, the permeability of PP-*g*-PPEGMA should be studied and the material should not be permeable to water or any gasses. Finally, a stability study should be set up which should be as close to reality as possible. PEGMA should be grafted *from* PP containers and the modified containers should be compared with glass.

11 References

[1] A. Nayak, A.K. Dutta, and G. Belfort, Surface-enhanced nucleation of insulin amyloid fibrillation, Biochem. Biophys. Res. Commun., 369 (2008) 303-307.

[2] H. Thurow and K. Geisen, Stabilisation of Dissolved Proteins against Denaturation at Hydrophobic Interfaces, Diabetologia, 27 (1984) 212-2.

[3] M.I. Smith, J.S. Sharp, and C.J. Roberts, Nucleation and growth of insulin fibrils in bulk solution and at hydrophobic polystyrene surfaces, Biophys. J., 93 (2007) 2143-2151.

[4] M. Zhu, P.O. Souillac, C. Ionescu-Zanetti, S.A. Carter, and A.L. Fink, Surface-catalyzed amyloid fibril formation, J. Biol. Chem., 277 (2002) 50914-50922.

[5] J. Brange, L. Andersen, E.D. Laursen, G. Meyn, and E. Rasmussen, Toward understanding insulin fibrillation, J. Pharm. Sci., 86 (1997) 517-525.

[6] L. Nielsen, R. Khurana, A. Coats, S. Frokjaer, J. Brange, S. Vyas, V.N. Uversky, and A.L. Fink, Effect of environmental factors on the kinetics of insulin fibril formation: Elucidation of the molecular mechanism, Biochemistry, 40 (2001) 6036-6046.

[7] V. Sluzky, J.A. Tamada, A.M. Klibanov, and R. Langer, Kinetics of Insulin Aggregation in Aqueous Solutions upon Agitation in the Presence of Hydrophobic Surfaces, Proc. Natl. Acad. Sci. USA, 88 (1991) 9377-9381.

[8] B. Vestergaard, M. Groenning, M. Roessle, J.S. Kastrup, M. van de Weert, J.M. Flink, S. Frokjaer, M. Gajhede, and D.I. Svergun, A helical structural nucleus is the primary elongating unit of insulin amyloid fibrils, Plos Biology, 5 (2007) 1089-1097.

[9] T. Arnebrant and T. Nylander, Adsorption of Insulin on Metal-Surfaces in Relation to Association Behavior, J. Colloid Interface Sci., 122 (1988) 557-566.

[10] P. Nilsson, T. Nylander, and S. Havelund, Adsorption of Insulin on Solid-Surfaces in Relation to the Surface-Properties of the Monomeric and Oligomeric Forms, J. Colloid Interface Sci., 144 (1991) 145-152.

[11] J. Senstius, C. Poulsen, and A. Hvass, Comparison of in vitro stability for insulin aspart and insulin glulisine during simulated use in infusion pumps, Diabetes Technol. Ther., 9 (2007) 517-521.

[12] J.H. Lee, H.B. Lee, and J.D. Andrade, Blood Compatibility of Polyethylene Oxide Surfaces, Prog. Polym. Sci., 20 (1995) 1043-1079.

[13] D.L. Elbert and J.A. Hubbell, Surface treatments of polymers for biocompatibility, Annu. Rev. Mater. Sci., 26 (1996) 365-394.

[14] M. Malmsten, K. Emoto, and J.M. Van Alstine, Effect of chain density on inhibition of protein adsorption by poly(ethylene glycol) based coatings, J. Colloid Interface Sci., 202 (1998) 507-517.

[15] J. Groll, Z. Ademovic, T. Ameringer, D. Klee, and M. Moeller, Comparison of Coatings from Reactive Star Shaped PEG-stat-PPG Prepolymers and Grafted Linear PEG for Biological ans Medical Applications, Biomacromolecules, 6 (2005) 956-962.

[16] K.L. Prime and G.M. Whitesides, Adsorption of Proteins Onto Surfaces Containing End-Attached Oligo(Ethylene Oxide) - A Model System Using Self-Assembled Monolayers, J. Am. Chem. Soc., 115 (1993) 10714-10721.

[17] K. Bergstrom, E. Osterberg, K. Holmberg, A.S. Hoffman, T.P. Schuman, A. Kozlowski, and J.M. Harris, Effects of Branching and Molecular-Weight of Surface-Bound Poly(Ethylene Oxide) on Protein Rejection, J. Biomat. Sci. -Polym. E., 6 (1994) 123-132.

[18] M.E. Norman, P. Williams, and L. Illum, Human Serum-Albumin As A Probe for Surface Conditioning (Opsonization) of Block Copolymer-Coated Microspheres, Biomaterials, 13 (1992) 841-849.

[19] J.S. Tan, D.E. Butterfield, C.L. Voycheck, K.D. Caldwell, and J.T. Li, Surface Modification of Nanoparticles by Peo Ppo Block-Copolymers to Minimize Interactions with Blood Components and Prolong Blood-Circulation in Rats, Biomaterials, 14 (1993) 823-833.

[20] K. Kato, S. Sano, and Y. Ikada, Protein Adsorption Onto Ionic Surfaces, Colloids Surf. , B, 4 (1995) 221-230.

[21] N.P. Desai and J.A. Hubbell, Solution Technique to Incorporate Polyethylene Oxide and Other Water-Soluble Polymers onto Surfaces of Polymeric Biomaterials, Biomaterials, 12 (1991) 144-1.

[22] N.P. Desai and J.A. Hubbell, Biological Responses to Polyethylene Oxide Modified Polyethylene Terephthalate Surfaces, J. Biomed. Mater. Res., 25 (1991) 829-843.

[23] S.G. Shafer and J.M. Harris, Preparation of Cyanuric-Chloride Activated Poly(Ethylene Glycol), J. Polym. Sci. , Part A: Polym. Chem., 24 (1986) 375-378.

[24] X.P. Zou, E.T. Kang, and K.G. Neoh, Plasma-induced graft polymerization of poly(ethylene glycol) methyl ether methacrylate on poly (tetrafluoroethylene) films for reduction in protein adsorption, Surf. Coat. Technol., 149 (2002) 119-128.

[25] R.B. Timmons and A.J. Griggs, Pulsed Plasma Polymerizations, in: H. Biederman (Ed.), Plasma Polymer Films, Imperial College Press, London, 2004, pp. 217-245.

[26] H. Biederman, Introduction, in: H. Biederman (Ed.), Plasma Polymer Films, Imperial College Press, London, 2004, pp. 13-24.

[27] F. Zhou and W.T.S. Huck, Surface grafted polymer brushes as ideal building blocks for "smart" surfaces, Phys. Chem. Chem. Phys., 8 (2006) 3815-3823.

[28] J.S. Wang and K. Matyjaszewski, Controlled Living Radical Polymerization - Atom-Transfer Radical Polymerization in the Presence of Transition-Metal Complexes, J. Am. Chem. Soc., 117 (1995) 5614-5615.

[29] M. Kato, M. Kamigaito, M. Sawamoto, and T. Higashimura, Polymerization of Methyl-Methacrylate with the Carbon-Tetrachloride Dichlorotris(Triphenylphosphine)Ruthenium(Ii) Methylaluminum Bis(2,6-Di-Tert-Butylphenoxide) Initiating System - Possibility of Living Radical Polymerization, Macromolecules, 28 (1995) 1721-1723.

[30] WO 9630421A1 (Matyjaszewski, K., Wang, J.) 3 October 1996.

[31] C.P. Chen, B.T. Ko, S.L. Lin, M.Y. Hsu, and C. Ting, Hydrophilic polymer supports grafted by poly(ethylene glycol) derivatives via atom transfer radical polymerization, Polymer, 47 (2006) 6630-6635.

[32] Z.P. Cheng, X.L. Zhu, Z.L. Shi, K.G. Neoh, and E.T. Kang, Polymer microspheres with permanent antibacterial surface from surface-initiated atom transfer radical polymerization, Ind. Eng. Chem. Res., 44 (2005) 7098-7104.

[33] Z.P. Cheng, X.L. Zhu, Z.L. Shi, K.G. Neoh, and E.T. Kang, Polymer microspheres with permanent antibacterial surface from surface-initiated atom transfer radical polymerization of 4-vinylpyridine and quaternization, Surf. Rev. Lett., 13 (2006) 313-318.

[34] A. Mizutani, A. Kikuchi, M. Yamato, H. Kanazawa, and T. Okano, Preparation of thermoresponsive polymer brush surfaces and their interaction with cells, Biomaterials, 29 (2008) 2073-2081.

[35] Y.W. Chen, D.M. Liu, Q.L. Deng, X.H. He, and X.F. Wang, Atom transfer radical polymerization directly from poly(vinylidene fluoride): Surface and antifouling properties, J. Polym. Sci. , Part A: Polym. Chem., 44 (2006) 3434-3443.

[36] J.F. Hester, P. Banerjee, Y.Y. Won, A. Akthakul, M.H. Acar, and A.M. Mayes, ATRP of amphiphilic graft copolymers based on PVDF and their use as membrane additives, Macromolecules, 35 (2002) 7652-7661.

[37] C.J. Fristrup, K. Jankova, and S. Hvilsted, Surface-initiated atom transfer radical polymerization-a technique to develop biofunctional coatings, Soft Matter, 5 (2009) 4623-4634.

[38] P. Liu, Modification of polymeric materials via surface-initiated controlled/"living" radical polymerization, E-Polymers, (2007).

[39] D. Roy, M. Semsarilar, J.T. Guthrie, and S. Perrier, Cellulose modification by polymer grafting: a review, Chem. Soc. Rev., 38 (2009) 2046-2064.

[40] B. Radhakrishnan, R. Ranjan, and W.J. Brittain, Surface initiated polymerizations from silica nanoparticles, Soft Matter, 2 (2006) 386-396.

[41] C.M. Homenick, G. Lawson, and A. Adronov, Polymer grafting of carbon nanotubes using living free-radical polymerization, Polymer Reviews, 47 (2007) 265-290.

[42] R. Barbey, L. Lavanant, D. Paripovic, N. Schuwer, C. Sugnaux, S. Tugulu, and H.A. Klok, Polymer Brushes via Surface-Initiated Controlled Radical Polymerization: Synthesis, Characterization, Properties, and Applications, Chem. Rev., 109 (2009) 5437-5527.

[43] F.J. Xu, K.G. Neoh, and E.T. Kang, Bioactive surfaces and biomaterials via atom transfer radical polymerization, Prog. Polym. Sci., 34 (2009) 719-761.

[44] N. Singh, J. Wang, M. Ulbricht, S.R. Wickramasinghe, and S.M. Husson, Surface-initiated atom transfer radical polymerization: A new method for preparation of polymeric membrane adsorbers, J. Membr. Sci., 309 (2008) 64-72.

[45] S.B. Lee, R.R. Koepsel, S.W. Morley, K. Matyjaszewski, Y.J. Sun, and A.J. Russell, Permanent, nonleaching antibacterial surfaces. 1. Synthesis by atom transfer radical polymerization, Biomacromolecules, 5 (2004) 877-882.

[46] D. Bozukova, C. Pagnoulle, M.C. Pauw-Gillet, N. Ruth, R. Jerome, and C. Jerome, Imparting antifouling properties of poly(2-hydroxyethyl methacrylate) hydrogels by grafting poly(oligoethylene glycol methyl ether acrylate), Langmuir, 24 (2008) 6649-6658.

[47] B.R. Coad, B.M. Steels, J.N. Kizhakkedathu, D.E. Brooks, and C.A. Haynes, The influence of grafted polymer architecture and fluid hydrodynamics on protein separation by entropic interaction chromatography, Biotechnol. Bioeng., 97 (2007) 574-587.

[48] F.J. Xu, J.P. Zhao, E.T. Kang, K.G. Neoh, and J. Li, Functionalization of nylon membranes via surface-initiated atom-transfer radical polymerization, Langmuir, 23 (2007) 8585-8592.

[49] J.Y. Huang, H. Murata, R.R. Koepsel, A.J. Russell, and K. Matyjaszewski, Antibacterial polypropylene via surface-initiated atom transfer radical polymerization, Biomacromolecules, 8 (2007) 1396-1399.

[50] L. Li, Z.J. Ke, G.P. Yan, and J.Y. Wu, Polyimide films with antibacterial surfaces from surface-initiated atom-transfer radical polymerization, Polym. Int., 57 (2008) 1275-1280.

[51] G.Q. Zhai, E.T. Kang, and K.G. Neoh, Inimer graft-copolymerized poly(vinylidene fluoride) for the preparation of arborescent copolymers and "surface-active" copolymer membranes, Macromolecules, 37 (2004) 7240-7249.

[52] G.Q. Zhai, Z.L. Shi, E.T. Kang, and K.G. Neoh, Surface-initiated atom transfer radical polymerization on poly(vinylidene fluoride) membrane for antibacterial ability, Macromol. Biosci., 5 (2005) 974-982.

[53] X.W. Jiang, H.Y. Chen, G. Galvan, M. Yoshida, and J. Lahann, Vapor-based initiator coatings for atom transfer radical polymerization, Adv. Funct. Mater., 18 (2008) 27-35.

[54] W. Jakubowski and K. Matyjaszewski, Activators regenerated by electron transfer for atom-transfer radical polymerization of (meth)acrylates and related block copolymers, Angew. Chem. Int. Ed. Engl., 45 (2006) 4482-4486.

[55] K. Min, H.F. Gao, and K. Matyjaszewski, Use of ascorbic acid as reducing agent for synthesis of well-defined polymers by ARGET ATRP, Macromolecules, 40 (2007) 1789-1791.

[56] W.A. Braunecker and K. Matyjaszewski, Controlled/living radical polymerization: Features, developments, and perspectives, Prog. Polym. Sci., 32 (2007) 93-146.

[57] K. Matyjaszewski, H.C. Dong, W. Jakubowski, J. Pietrasik, and A. Kusumo, Grafting from surfaces for "Everyone": ARGET ATRP in the presence of air, Langmuir, 23 (2007) 4528-4531.

[58] M. Ignatova, S. Voccia, B. Gilbert, N. Markova, D. Cossement, R. Gouttebaron, R. Jerome, and C. Jerome, Combination of electrografting and atom-transfer radical polymerization for making the stainless steel surface antibacterial and protein antiadhesive, Langmuir, 22 (2006) 255-262.

[59] I. Cringus-Fundeanu, J. Luijten, H.C. van der Mei, H.J. Busscher, and A.J. Schouten, Synthesis and characterization of surface-grafted polyacrylamide brushes and their inhibition of microbial adhesion, Langmuir, 23 (2007) 5120-5126.

[60] T. Tsukagoshi, Y. Kondo, and N. Yoshino, Protein adsorption on polymer-modified silica particle surface, Colloids Surf. , B, 54 (2007) 101-107.

[61] X.Y. Huang and M.J. Wirth, Surface-initiated radical polymerization on porous silica, Anal. Chem., 69 (1997) 4577-4580.

[62] X.Y. Huang, L.J. Doneski, and M.J. Wirth, Make ultrathin films using surface-confined living radical polymerization, Chemtech, 28 (1998) 19-25.

[63] S. Kurosawa, H. Aizawa, Z.A. Talib, B. Atthoff, and J. Hilborn, Synthesis of tethered-polymer brush by atom transfer radical polymerization from a plasma-polymerized-film-coated quartz crystal microbalance and its application for immunosensors, Biosens. Bioelectron., 20 (2004) 1165-1176.

[64] V.P. Hoven, M. Srinanthakul, Y. Iwasaki, R. Iwata, and S. Kiatkamjornwong, Polymer brushes in nanopores surrounded by silicon-supported tris(trimethylsiloxy)silyl monolayers, J. Colloid Interface Sci., 314 (2007) 446-459.

[65] Z. Zhang, S.F. Chen, and S.Y. Jiang, Dual-functional biomimetic materials: Nonfouling poly(carboxybetaine) with active functional groups for protein immobilization, Biomacromolecules, 7 (2006) 3311-3315.

[66] Z. Zhang, M. Zhang, S.F. Chen, T.A. Horbetta, B.D. Ratner, and S.Y. Jiang, Blood compatibility of surfaces with superlow protein adsorption, Biomaterials, 29 (2008) 4285-4291.

[67] H.W. Duan, M. Kuang, G. Zhang, D.Y. Wang, D.G. Kurth, and H. Mohwald, pH-Responsive capsules derived from nanocrystal templating, Langmuir, 21 (2005) 11495-11499.

[68] A. Kusumo, L. Bombalski, Q. Lin, K. Matyjaszewski, J.W. Schneider, and R.D. Tilton, High capacity, charge-selective protein uptake by polyelectrolyte brushes, Langmuir, 23 (2007) 4448-4454.

[69] F. Zhang, F.J. Xu, E.T. Kang, and K.G. Neoh, Modification of titanium via surface-initiated atom transfer radical polymerization (ATRP), Ind. Eng. Chem. Res., 45 (2006) 3067-3073.

[70] F.J. Xu, S.P. Zhong, L.Y.L. Yung, Y.W. Tong, E.T. Kang, and K.G. Neoh, Thermoresponsive comb-shaped copolymer-Si(100) hybrids for accelerated temperature-dependent cell detachment, Biomaterials, 27 (2006) 1236-1245.

[71] J.S. Huang, X.T. Li, Y.H. Zheng, Y. Zhang, R.Y. Zhao, X.C. Gao, and H.S. Yan, Immobilization of penicillin G acylase on poly[(glycidyl methacrylate)-co-(glycerol monomethacrylate)]-grafted magnetic microspheres, Macromol. Biosci., 8 (2008) 508-515.

[72] F.J. Xu, Q.J. Cai, Y.L. Li, E.T. Kang, and K.G. Neoh, Covalent immobilization of glucose oxidase on well-defined poly(glycidyl methacrylate)-Si(111) hybrids from surface-initiated atom-transfer radical polymerization, Biomacromolecules, 6 (2005) 1012-1020.

[73] Y. Mei, T. Wu, C. Xu, K.J. Langenbach, J.T. Elliott, B.D. Vogt, K.L. Beers, E.J. Amis, and N.R. Washburn, Tuning cell adhesion on gradient poly(2-hydroxyethyl methacrylate)-grafted surfaces, Langmuir, 21 (2005) 12309-12314.

[74] S. Tugulu, A. Arnold, I. Sielaff, K. Johnsson, and H.A. Klok, Protein-functionalized polymer brushes, Biomacromolecules, 6 (2005) 1602-1607.

[75] S. Tugulu, P. Silacci, N. Stergiopulos, and H.A. Klok, RGD - Functionalized polymer brushes as substrates for the integrin specific adhesion of human umbilical vein endothelial cells, Biomaterials, 28 (2007) 2536-2546.

[76] X.H. Lou and L. He, DNA-accelerated atom transfer radical polymerization on a gold surface, Langmuir, 22 (2006) 2640-2646.

[77] X.H. Lou, C.Y. Wang, and L. He, Core-shell Au nanoparticle formation with DNA-polymer hybrid coatings using aqueous ATRP, Biomacromolecules, 8 (2007) 1385-1390.

[78] X.H. Lou and L. He, Surface passivation using oligo(ethylene glycol) in ATRP-assisted DNA detection, Sens. Actuators, B, 129 (2008) 225-230.

[79] G.O. Okelo and L. He, Cu(0) as the reaction additive in purge-free ATRP-assisted DNA detection, Biosens. Bioelectron., 23 (2007) 588-592.

[80] F.J. Xu, S.P. Zhong, L.Y.L. Yung, Y.W. Tong, E.T. Kang, and K.G. Neoh, Collagen-coupled poly(2-hydroxyethyl methacrylate)-Si(111) hybrid surfaces for cell immobilization, Tissue Eng., 11 (2005) 1736-1748.

[81] F. Zhang, Z.L. Shi, P.H. Chua, E.T. Kang, and K.G. Neoh, Functionalization of titanium surfaces via controlled living radical polymerization: From antibacterial surface to surface for osteoblast adhesion, Ind. Eng. Chem. Res., 46 (2007) 9077-9086.

[82] C. Yoshikawa, A. Goto, Y. Tsujii, N. Ishizuka, K. Nakanishi, and T. Fukuda, Sur-face interaction of well-defined, concentrated poly,(2-hydroxyethyl methacrylate) brushes with proteins, J. Polym. Sci. , Part A: Polym. Chem., 45 (2007) 4795-4803.

[83] F. Zhang, Z.B. Zhang, X.L. Zhu, E.T. Kang, and K.G. Neoh, Silk-functionalized titanium surfaces for enhancing osteoblast functions and reducing bacterial adhesion, Biomaterials, 29 (2008) 4751-4759.

[84] N. Ayres, D.J. Holt, C.F. Jones, L.E. Corum, and D.W. Grainger, Polymer Brushes Containing Sulfonated Sugar Repeat Units: Synthesis, Charaderization, and In Vitro Testing of Blood Coagulation

Activation, J. Polym. Sci. , Part A: Polym. Chem., 46 (2008) 7713-7724.

[85] Y. Zhou, S.X. Wang, B.J. Ding, and Z.M. Yang, Modification of magnetite nanoparticles via surface-initiated atom transfer radical polymerization (ATRP), Chem. Eng. J., 138 (2008) 578-585.

[86] T. Matrab, M.M. Chehimi, J.P. Boudou, F. Benedic, J. Wang, N.N. Naguib, and J.A. Carlisle, Surface functionalization of ultrananocrystalline diamond using atom transfer radical polymerization (ATRP) initiated by electro-grafted aryldiazonium salts, Diamond Relat. Mater., 15 (2006) 639-644.

[87] T. Matrab, M.M. Chehimi, C. Perruchot, A. Adenier, A. Guillez, M. Save, B. Charleux, E. Cabet-Deliry, and J. Pinson, Novel approach for metallic surface-initiated atom transfer radical polymerization using electrografted initiators based on aryl diazonium salts, Langmuir, 21 (2005) 4686-4694.

[88] W. Feng, S.P. Zhu, K. Ishihara, and J.L. Brash, Adsorption of fibrinogen and lysozyme on silicon grafted with poly(2-methacryloyloxyethyl phosphorylcholine) via surface-initiated atom transfer radical polymerization, Langmuir, 21 (2005) 5980-5987.

[89] W. Feng, J.L. Brash, and S.P. Zhu, Non-biofouling materials prepared by atom transfer radical polymerization grafting of 2-methacryloloxyethyl phosphorylcholine: Separate effects of graft density and chain length on protein repulsion, Biomaterials, 27 (2006) 847-855.

[90] R. Iwata, P. Suk-In, V.P. Hoven, A. Takahara, K. Akiyoshi, and Y. Iwasaki, Control of nanobiointerfaces generated from well-defined biomimetic polymer brushes for protein and cell manipulations, Biomacromolecules, 5 (2004) 2308-2314.

[91] W.K. Cho, B.Y. Kong, and I.S. Choi, Highly efficient non-biofouling coating of zwitterionic polymers: Poly((3-(methacryloylamino)propyl)-dimethyl(3-sulfopropyl)ammonium hydroxide), Langmuir, 23 (2007) 5678-5682.

[92] H.W. Ma, D.J. Li, X. Sheng, B. Zhao, and A. Chilkoti, Protein-resistant polymer coatings on silicon oxide by surface-initiated atom transfer radical polymerization, Langmuir, 22 (2006) 3751-3756.

[93] A.A. Brown, N.S. Khan, L. Steinbock, and W.T.S. Huck, Synthesis of oligo(ethylene glycol) methacrylate polymer brushes, Eur. Polym. J., 41 (2005) 1757-1765.

[94] G. Cheng, Z. Zhang, S.F. Chen, J.D. Bryers, and S.Y. Jiang, Inhibition of bacterial adhesion and biofilm formation on zwitterionic surfaces, Biomaterials, 28 (2007) 4192-4199.

[95] H.W. Ma, J.H. Hyun, P. Stiller, and A. Chilkoti, "Non-fouling" oligo(ethylene glycol)-functionalized polymer brushes synthesized by surface-initiated atom transfer radical polymerization, Adv. Mater., 16 (2004) 338-341.

[96] H.W. Ma, M. Wells, T.P. Beebe, and A. Chilkoti, Surface-initiated atom transfer radical polymerization of oligo(ethylene glycol) methyl methacrylate from a mixed self-assembled monolayer on gold, Adv. Funct. Mater., 16 (2006) 640-648.

[97] T. Tsukagoshi, Y. Kondo, and N. Yoshino, Surface modification of poly(oligoethylene oxide methacrylate) for resisting protein adsorption, Colloids Surf. , B, 54 (2007) 94-100.

[98] X.W. Fan, L.J. Lin, J.L. Dalsin, and P.B. Messersmith, Biomimetic anchor for surface-initiated polymerization from metal substrates, J. Am. Chem. Soc., 127 (2005) 15843-15847.

[99] X.W. Fan, L.J. Lin, and P.B. Messersmith, Cell fouling resistance of polymer brushes grafted from Ti substrates by surface-initiated polymerization: Effect of ethylene glycol side chain length, Biomacromolecules, 7 (2006) 2443-2448.

[100] B.S. Lee, J.K. Lee, W.J. Kim, Y.H. Jung, S.J. Sim, J. Lee, and I.S. Choi, Surface-initiated, atom transfer radical polymerization of oligo(ethylene glycol) methyl ether methacrylate and subsequent click chemistry for bioconjugation, Biomacromolecules, 8 (2007) 744-749.

[101] F.J. Xu, H.Z. Li, J. Li, Y.H.E. Teo, C.X. Zhu, E.T. Kang, and K.G. Neoh, Spatially well-defined binary brushes of poly(ethylene glycol)s for micropatterning of active proteins on anti-fouling surfaces, Biosens. Bioelectron., 24 (2008) 773-780.

[102] Y. Yao, Y.Z. Ma, M. Qin, X.J. Ma, C. Wang, and X.Z. Feng, NHS-ester functionalized poly(PEGMA) brushes on silicon surface for covalent protein immobilization, Colloids Surf. , B, 66 (2008) 233-239.

[103] D.J. Kim, B. Kong, Y.H. Jung, K.S. Kim, W.J. Kim, K.B. Lee, S.M. Kang, S. Jeon, and I.S. Choi, Formation of thermoresponsive surfaces by surface-initiated, aqueous atom-transfer radical polymerization of N-isopropylacrylamide: Application to cell culture, Bull. Korean Chem. Soc., 25 (2004) 1629-1630.

[104] L.H. Li, Y. Zhu, B. Li, and C.Y. Gao, Fabrication of Thermoresponsive Polymer Gradients for Study of Cell Adhesion and Detachment, Langmuir, 24 (2008) 13632-13639.

[105] F.J. Xu, S.P. Zhong, L.Y.L. Yung, E.T. Kang, and K.G. Neoh, Surface-active and stimuli-responsive polymer-Si(100) hybrids from surface-initiated atom transfer radical polymerization for control of cell adhesion, Biomacromolecules, 5 (2004) 2392-2403.

[106] S.C. Wuang, K.G. Neoh, E.T. Kang, D.W. Pack, and D.E. Leckband, Heparinized magnetic nanoparticles: In-vitro assessment for biomedical applications, Adv. Funct. Mater., 16 (2006) 1723-1730.

[107] N. Idota, A. Kikuchi, J. Kobayashi, Y. Akiyama, and T. Okano, Thermal modulated interaction of aqueous steroids using polymer-grafted capillaries, Langmuir, 22 (2006) 425-430.

[108] K. Nagase, J. Kobayashi, A. Kikuchi, Y. Akiyama, H. Kanazawa, and T. Okano, Interfacial property modulation of thermoresponsive polymer brush surfaces and their interaction with biomolecules, Langmuir, 23 (2007) 9409-9415.

[109] K. Nagase, J. Kobayashi, A.I. Kikuchi, Y. Akiyama, H. Kanazawa, and T. Okano, Effects of graft densities and chain lengths on separation of bioactive compounds by nanolayered thermoresponsive polymer brush surfaces, Langmuir, 24 (2008) 511-517.

[110] Z.Y. Zhou, S.M. Zhu, and D. Zhang, Grafting of thermo-responsive polymer inside mesoporous silica with large pore size using ATRP and investigation of its use in drug release, J. Mater. Chem., 17 (2007) 2428-2433.

[111] T. Tsukagoshi, Y. Kondo, and N. Yoshino, Preparation of thin polymer films with controlled drug release, Colloids Surf. , B, 57 (2007) 219-225.

[112] F.X. Hu, K.G. Neoh, L. Cen, and E.T. Kang, Cellular response to magnetic nanoparticles "PEGylated" via surface-initiated atom transfer radical polymerization, Biomacromolecules, 7 (2006) 809-816.

[113] S. Tugulu and H.A. Klok, Stability and nonfouling properties of poly(poly(ethylene glycol) methacrylate) brushes-under cell culture conditions, Biomacromolecules, 9 (2008) 906-912.

[114] B.S. Lee, Y.S. Chi, K.B. Lee, Y.G. Kim, and I.S. Choi, Functionalization of poly(oligo(ethylene glycol)methacrylate) films on gold and Si/SiO2 for immobilization of proteins and cells: SPR and QCM studies, Biomacromolecules, 8 (2007) 3922-3929.

[115] N. Singh, X.F. Cui, T. Boland, and S.M. Husson, The role of independently variable grafting density and layer thickness of polymer nanolayers on peptide adsorption and cell adhesion, Biomaterials, 28 (2007) 763-771.

[116] L. Li, G.P. Yan, J.Y. Wu, X.H. Yu, and Q.Z. Guo, Surface-initiated atom-transfer radical polymerization from polyimide films and their anti-fouling properties, J. Macromol. Sci. Pure, 45 (2008) 828-832.

[117] F.J. Xu, Y.L. Li, E.T. Kang, and K.G. Neoh, Heparin-coupled poly(poly(ethylene glycol) monomethacrylate)-Si(111) hybrids and their blood compatible surfaces, Biomacromolecules, 6 (2005) 1759-1768.

[118] G.Z. Li, H. Xue, G. Cheng, S.F. Chen, F.B. Zhang, and S.Y. Jiang, Ultralow Fouling Zwitterionic Polymers Grafted from Surfaces Covered with an Initiator via an Adhesive Mussel Mimetic Linkage, J. Phys. Chem. B, 112 (2008) 15269-15274.

[119] W. Yang, S.F. Chen, G. Cheng, H. Vaisocherova, H. Xue, W. Li, J.L. Zhang, and S.Y. Jiang, Film thickness dependence of protein adsorption from blood serum and plasma onto poly(sulfobetaine)-grafted surfaces, Langmuir, 24 (2008) 9211-9214.

[120] R. Dong, S. Krishnan, B.A. Baird, M. Lindau, and C.K. Ober, Patterned biofunctional poly(acrylic acid) brushes on silicon surfaces, Biomacromolecules, 8 (2007) 3082-3092.

[121] E. Unsal, B. Elmas, B. Caglayan, M. Tuncel, S. Patir, and A. Tuncel, Preparation of an ion-exchange chromatographic support by a "grafting from" strategy based on atom transfer radical polymerization, Anal. Chem., 78 (2006) 5868-5875.

[122] X. Li, X.L. Wei, and S.M. Husson, Thermodynamic studies on the adsorption of fibronectin adhesion-promoting peptide on nanothin films of poly(2-vinylpyridine) by SPR, Biomacromolecules, 5 (2004) 869-876.

[123] D. Plackett, K. Jankova, H. Egsgaard, and S. Hvilsted, Modification of jute fibers with polystyrene via atom transfer radical polymerization, Biomacromolecules, 6 (2005) 2474-2484.

[124] A. Carlmark and E.E. Malmstrom, ATRP grafting from cellulose fibers to create block-copolymer grafts, Biomacromolecules, 4 (2003) 1740-1745.

[125] M. Ejaz, S. Yamamoto, K. Ohno, Y. Tsujii, and T. Fukuda, Controlled graft polymerization of methyl methacrylate on silicon substrate by the combined use of the Langmuir-Blodgett and atom transfer radical polymerization techniques, Macromolecules, 31 (1998) 5934-5936.

[126] V. Castelvetro, M. Geppi, S. Giaiacopi, and G. Mollica, Cotton fibers encapsulated with homo- and block copolymers: Synthesis by the atom transfer radical polymerization grafting-from technique and solid-state NMR dynamic investigations, Biomacromolecules, 8 (2007) 498-508.

[127] W.X. Huang, J.B. Kim, M.L. Bruening, and G.L. Baker, Functionalization of surfaces by water-accelerated atom-transfer radical polymerization of hydroxyethyl methacrylate and subsequent derivatization, Macromolecules, 35 (2002) 1175-1179.

[128] M.J. Cannon and D.G. Myszka, Surface Plasmon Resonance, in: W. Jiskoot, Crommelin, and D.J.A (Eds.), Biotechnology: Pharmaceutical Aspects, Vol. 3. American Association of Pharmaceutical Scientists, Arlington, Va, 2005, pp. 527-544.

[129] J. Wegener, A. Janshoff, and C. Steinem, The quartz crystal microbalance as a novel means to study cell-substrate interactions in situ, Cell Biochem. Biophys., 34 (2001) 121-151.

[130] C.K. O'Sullivan and G.G. Guilbault, Commercial quartz crystal microbalances - theory and applications, Biosens. Bioelectron., 14 (1999) 663-670.

[131] M. Müller, Introduction to Confocal Fluorescence Microscopy, SPIE Press, Washington 2006.

[132] J. MarchandBrynaert, G. Pantano, and O. Noiset, Surface fluorination of PEEK film by selective wet-chemistry, Polymer, 38 (1997) 1387-1394.

[133] O. Noiset, Y.J. Schneider, and J. Marchand-Brynaert, Surface modification of poly(aryl ether ether ketone) (PEEK) film by covalent

coupling of amines and amino acids through a spacer arm, J. Polym. Sci. , Part A: Polym. Chem., 35 (1997) 3779-3790.

[134] O. Noiset, C. Henneuse, Y.J. Schneider, and J. Marchand-Brynaert, Surface reduction of poly(aryl ether ether ketone) film: UV spectrophotometric, H-3 radiochemical, and X-ray photoelectron spectroscopic assays of the hydroxyl functions, Macromolecules, 30 (1997) 540-548.

[135] O. Noiset, Y.J. Schneider, and J. Marchand-Brynaert, Fibronectin adsorption or and covalent grafting on chemically modified PEEK film surfaces, J. Biomat. Sci. -Polym. E., 10 (1999) 657-677.

[136] O. Noiset, Y.J. Schneider, and J. Marchand-Brynaert, Adhesion and growth of CaCo2 cells on surface-modified PEEK substrata, J. Biomat. Sci. -Polym. E., 11 (2000) 767-786.

[137] S.M. Kurtz and J.N. Devine, PEEK biomaterials in trauma, orthopedic, and spinal implants, Biomaterials, 28 (2007) 4845-4869.

[138] A. Carlmark and E. Malmstrom, Atom transfer radical polymerization from cellulose fibers at ambient temperature, J. Am. Chem. Soc., 124 (2002) 900-901.

[139] K. Rechendorff, M.B. Hovgaard, M. Foss, V.P. Zhdanov, and F. Besenbacher, Enhancement of protein adsorption induced by surface roughness, Langmuir, 22 (2006) 10885-10888.

[140] J.F. Lutz, Polymerization of oligo(ethylene glycol) (meth)acrylates: Toward new generations of smart biocompatible materials, J. Polym. Sci. , Part A: Polym. Chem., 46 (2008) 3459-3470.

[141] C.J. Fristrup, K. Jankova, and S. Hvilsted, Hydrophilization of Poly(ether ether ketone) Films by Surface-Initiated Atom Transfer radical Polymerization, Polym. Chem., 1 (2010) 1696-1701.

[142] J. Brange, Stability of insulin - studies on the physical and chemical stability of insulin in pharmaceutical formulation, Kluwer Academic Publishers, Boston 1994.

[143] A. Hvass, M. Hach, and M.U. Jars, Complementary analytical HPLC methods for insulin-related degradation products, American Biotech. Lab., 21 (2003) 8-12.

[144] M.U. Jars, A. Hvass, and D. Waaben, Insulin aspart (Asp(B28) human insulin) derivatives formed in pharmaceutical solutions, Pharm. Res., 19 (2002) 621-628.

[145] J.L. Whittingham, D.J. Edwards, A.A. Antson, J.M. Clarkson, and C.G. Dodson, Interactions of phenol and m-cresol in the insulin hexamer, and their effect on the association properties of B28 Pro -> Asp insulin analogues, Biochemistry, 37 (1998) 11516-11523.

[146] U. Derewenda, Z. Derewenda, E.J. Dodson, G.G. Dodson, C.D. Reynolds, G.D. Smith, C. Sparks, and D. Swenson, Phenol Stabilizes More Helix in A New Symmetrical Zinc Insulin Hexamer, Nature, 338 (1989) 594-596.

[147] V. Fodera, M. Groenning, V. Vetri, F. Librizzi, S. Spagnolo, C. Cornett, L. Olsen, M. van de Weert, and M. Leone, Thioflavin T Hydroxylation at Basic pH and Its Effect on Amyloid Fibril Detection, J. Phys. Chem. B, 112 (2008) 15174-15181.

[148] V. Tougu, A. Karafin, K. Zovo, R.S. Chung, C. Howells, A.K. West, and P. Palumaa, Zn(II)- and Cu(II)-induced non-fibrillar aggregates of amyloid-beta (1-42) peptide are transformed to amyloid fibrils, both spontaneously and under the influence of metal chelators, J. Neurochem., 110 (2009) 1784-1795.

[149] V.N. Uversky, J. Li, and A.L. Fink, Metal-triggered structural transformations, aggregation, and fibrillation of human alpha-synuclein - A possible molecular link between Parkinson's disease and heavy metal exposure, J. Biol. Chem., 276 (2001) 44284-44296.

[150] Y. Yoshiike, K. Tanemura, O. Murayama, T. Akagi, M. Murayama, S. Sato, X.Y. Sun, N. Tanaka, and A. Takashima, New insights on how metals disrupt amyloid beta-aggregation and their effects on amyloid-beta cytotoxicity, J. Biol. Chem., 276 (2001) 32293-32299.